

# Mechanistic Investigation of Intramolecular Aminoalkene and Aminoalkyne Hydroamination/Cyclization Catalyzed by Highly Electrophilic, Tetravalent Constrained Geometry 4d and 5f Complexes. Evidence for an M–N $\sigma$ -Bonded Insertive Pathway

Bryan D. Stubbert and Tobin J. Marks\*

Contribution from the Department of Chemistry, Northwestern University,  
Evanston, Illinois 60208-3113

Received October 24, 2006; E-mail: t-marks@northwestern.edu

**Abstract:** A mechanistic study of intramolecular hydroamination/cyclization catalyzed by tetravalent organoactinide and organozirconium complexes is presented. A series of selectively substituted constrained geometry complexes, (CGC)M(NR<sub>2</sub>)Cl (CGC = [Me<sub>2</sub>Si( $\eta^5$ -Me<sub>4</sub>C<sub>5</sub>)(tBuN)]<sup>2-</sup>; M = Th, **1-CI**; U, **2-CI**; R = SiMe<sub>3</sub>; M = Zr, R = Me, **3-CI**) and (CGC)An(NMe<sub>2</sub>)OAr (An = Th, **1-OAr**; An = U, **2-OAr**), has been prepared via in situ protodeamination (complexes **1–2**) or salt metathesis (**3-CI**) in high purity and excellent yield and is found to be active precatalysts for intramolecular primary and secondary aminoalkyne and aminoalkene hydroamination/cyclization. Substrate reactivity trends, rate laws, and activation parameters for cyclizations mediated by these complexes are virtually identical to those of more conventional (CGC)-MR<sub>2</sub> (M = Th, R = NMe<sub>2</sub>, **1**; M = U, R = NMe<sub>2</sub>, **2**; M = Zr, R = Me, **3**), (Me<sub>2</sub>SiCp''<sub>2</sub>)UBr<sub>2</sub> (Cp'' =  $\eta^5$ -Me<sub>4</sub>C<sub>5</sub>; Bn = CH<sub>2</sub>Ph, **4**), Cp''<sub>2</sub>AnR<sub>2</sub> (Cp' =  $\eta^5$ -Me<sub>5</sub>C<sub>5</sub>; R = CH<sub>2</sub>SiMe<sub>3</sub>; An = Th, **5**, U, **6**), and analogous organolanthanide complexes. Deuterium KIEs measured at 25 °C in C<sub>6</sub>D<sub>6</sub> for aminoalkene D<sub>2</sub>NCH<sub>2</sub>C(CH<sub>3</sub>)<sub>2</sub>-CH<sub>2</sub>CHCH<sub>2</sub> (**11-d<sub>2</sub>**) with precatalysts **2** and **2-CI** indicate that  $k_H/k_D = 3.3(5)$  and  $2.6(4)$ , respectively. Together, the data provide strong evidence in these systems for turnover-limiting C–C insertion into an M–N(H)R  $\sigma$ -bond in the transition state. Related complexes (Me<sub>2</sub>SiCp''<sub>2</sub>)U(Br)(Cl) (**4-CI**) and Cp''<sub>2</sub>An(R)(Cl) (R = CH<sub>2</sub>(SiMe<sub>3</sub>); An = Th, **5-CI**; An = U, **6-CI**) are also found to be effective precatalysts for this transformation. Additional arguments supporting M–N(H)R intermediates vs M=NR intermediates are presented.

## Introduction

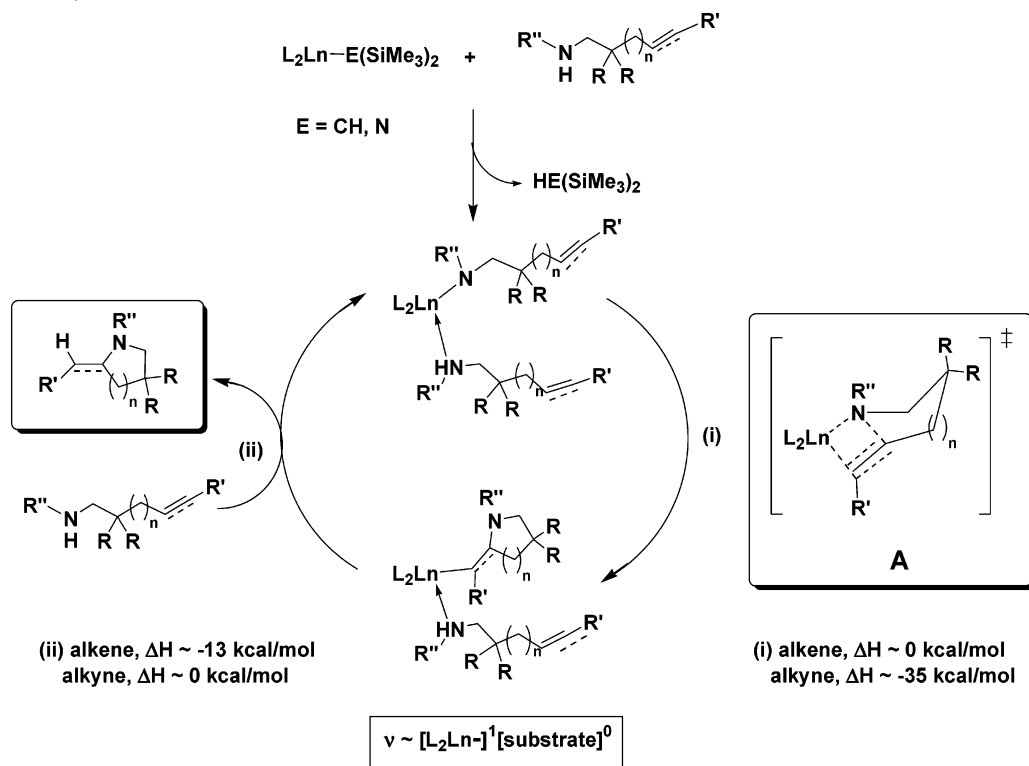
Hydroamination (HA), the atom-economical addition of an N–H bond across a C–C unsaturation,<sup>1</sup> is an important synthetic methodology for regiospecific C–N bond formation, a topic of considerable academic and industrial interest.<sup>2</sup> Research on this transformation pervades the Periodic Table,<sup>1</sup> with extensively studied organolanthanide-catalyzed intramolecular HA/cyclization playing a prominent role,<sup>3,4</sup> typically displaying near-quantitative yields in addition to high regio- and

diastereoselectivities (>95%)<sup>1d</sup> and with enantioselectivities as high as 95%.<sup>4b</sup> Mechanistic experiments with rigorously trivalent lanthanide (Ln) catalysts on intramolecular aminoalkene,<sup>3v,w</sup>

- (1) For general hydroamination reviews, see: (a) Odom, A. L. *Dalton Trans.* **2005**, 225–233. (b) Hultzsck, K. C. *Adv. Synth. Catal.* **2005**, *347*, 367–391. (c) Hultzsck, K. C.; Gribkov, D. V.; Hampel, F. J. *Organomet. Chem.* **2005**, *690*, 4441–4452. (d) Hong, S.; Marks, T. J. *Acc. Chem. Res.* **2004**, *37*, 673–686. (e) Doye, S. *Synlett* **2004**, 1653–1672. (f) Beller, M.; Tillack, A.; Seayad, J. In *Transition Metals for Organic Synthesis*, 2nd ed.; Beller, M., Bolm, C., Eds.; Wiley-VCH: Weinheim, 2004; pp 91–141. (g) Roesky, P. W.; Mueller, T. E. *Angew. Chem., Int. Ed.* **2003**, *42*, 2708–2710. (h) Pohlki, F.; Doye, S. *Chem. Soc. Rev.* **2003**, *32*, 104–114. (i) Bytschkov, I.; Doye, S. *Eur. J. Org. Chem.* **2003**, 935–946. (j) Seayad, J.; Tillack, A.; Hartung, C. G.; Beller, M. *Adv. Synth. Catal.* **2002**, *344*, 795–813. (k) Togni, A. In *Catalytic Heterofunctionalization*; Togni, A., Gruetzmacher, H., Eds.; Wiley-VCH: New York, 2001; pp 91–141. (l) Nobis, M.; Drießen-Holscher, B. *Angew. Chem., Int. Ed.* **2001**, *40*, 3983–3985. (m) Eisen, M. S.; Straub, T.; Haskel, A. J. *Alloys Compd.* **1998**, *271*–273, 116–122. (n) Mueller, T. E.; Beller, M. *Chem. Rev.* **1998**, *98*, 675–703.
- (2) For general C–N bond-formation references, see: (a) Beller, M.; Seayad, J.; Tillack, A.; Jiao, H. *Angew. Chem., Int. Ed.* **2004**, *43*, 3368–3398. (b) Hartwig, J. F. *Science* **2002**, *297*, 1653–1654. (c) Beller, M.; Riermeier, T. H. *Transition Met. Org. Synth.* **1998**, *1*, 184–194. (d) Hegedus, L. S. *Angew. Chem., Int. Ed. Engl.* **1988**, *27*, 1113–1126.

- (3) (a) Motta, A.; Lanza, G.; Fragala, I. L.; Marks, T. J. *Organometallics* **2004**, *23*, 4097–4104. (b) Seyam, A. M.; Stubbert, B. D.; Jensen, T. R.; O'Donnell, J. J., III; Stern, C. L.; Marks, T. J. *Inorg. Chim. Acta* **2004**, *357*, 4029–4035. (c) Ryu, J.-S.; Marks, T. J.; McDonald, F. E. *J. Org. Chem.* **2004**, *69*, 1038–1052. (d) Hong, S.; Kawaoka, A. M.; Marks, T. J. *J. Am. Chem. Soc.* **2003**, *125*, 15878–15892. (e) Hong, S.; Tian, S.; Metz, M. V.; Marks, T. J. *J. Am. Chem. Soc.* **2003**, *125*, 14768–14783. (f) Ryu, J.-S.; Li, G. Y.; Marks, T. J. *J. Am. Chem. Soc.* **2003**, *125*, 12584–12605. (g) Hong, S.; Marks, T. J. *J. Am. Chem. Soc.* **2002**, *124*, 7886–7887. (h) Ryu, J.-S.; Marks, T. J.; McDonald, F. E. *Org. Lett.* **2001**, *3*, 3091–3094. (i) Arredondo, V. M.; Tian, S.; McDonald, F. E.; Marks, T. J. *J. Am. Chem. Soc.* **1999**, *121*, 3633–3639. (j) Arredondo, V. M.; McDonald, F. E.; Marks, T. J. *Organometallics* **1999**, *18*, 1949–1960. (k) Tian, S.; Arredondo, V. M.; Stern, C. L.; Marks, T. J. *Organometallics* **1999**, *18*, 2568–2570. (l) Arredondo, V. M.; McDonald, F. E.; Marks, T. J. *J. Am. Chem. Soc.* **1998**, *120*, 4871–4872. (m) Li, Y.; Marks, T. J. *J. Am. Chem. Soc.* **1998**, *120*, 1757–1771. (n) Roesky, P. W.; Stern, C. L.; Marks, T. J. *Organometallics* **1997**, *16*, 4705–4711. (o) Li, Y.; Marks, T. J. *J. Am. Chem. Soc.* **1996**, *118*, 9295–9306. (p) Li, Y.; Marks, T. J. *Organometallics* **1996**, *15*, 3770–3772. (q) Li, Y.; Marks, T. J. *J. Am. Chem. Soc.* **1996**, *118*, 707–708. (r) Giardello, M. A.; Conticello, V. P.; Brard, L.; Gagné, M. R.; Marks, T. J. *J. Am. Chem. Soc.* **1994**, *116*, 10241–10254. (s) Giardello, M. A.; Conticello, V. P.; Brard, L.; Sabat, M.; Rheingold, A. L.; Stern, C. L.; Marks, T. J. *J. Am. Chem. Soc.* **1994**, *116*, 10212–10240. (t) Li, Y.; Fu, P.-F.; Marks, T. J. *Organometallics* **1994**, *13*, 439–440. (u) Gagné, M. R.; Brard, L.; Conticello, V. P.; Giardello, M. A.; Stern, C. L.; Marks, T. J. *J. Am. Chem. Soc.* **1992**, *114*, 275–294. (v) Gagné, M. R.; Stern, C. L.; Marks, T. J. *J. Am. Chem. Soc.* **1992**, *114*, 275–294. (w) Gagné, M. R.; Marks, T. J. *J. Am. Chem. Soc.* **1989**, *111*, 4108–9. (x) Motta, A.; Lanza, G.; Fragala, I. L.; Marks, T. J. *Organometallics* **2006**, *25*, 5533–5539.

**Scheme 1.** Proposed  $\sigma$ -Bond Inertive Mechanism for Intramolecular Aminoalkene and Aminoalkyne HA/Cyclization Mediated by Trivalent Organolanthanide Complexes<sup>a</sup>



<sup>a</sup> The pathway proposed for  $L_2Ln^{3+}$ -catalyzed *intermolecular* HA is similar, also proceeding through an  $L_2Ln-N(H)R$   $\sigma$ -bonded species, leading to a transition state analogous to **A** (see ref 1d).

aminoalkyne,<sup>3m,o-q,t</sup> aminoallene,<sup>3i,j,l</sup> internal olefin,<sup>3c,h</sup> and aminodiene<sup>3d,g</sup> HA/cyclization generally argue for turnover-limiting C=C/C≡C insertion into an  $L_2Ln-N$   $\sigma$ -bond (Scheme 1). The observed rate law ( $v \sim [Ln]^1 [substrate]^0$ ), moderate  $\Delta H^\ddagger$ , and large negative  $\Delta S^\ddagger$  are consistent with a highly ordered, polar **A**-like transition state,<sup>1d</sup> as are DFT calculations implicating an  $L_2Ln[N(H)R](H_2NR)$  catalyst resting state and **A**-like species.<sup>3a,x,5</sup>

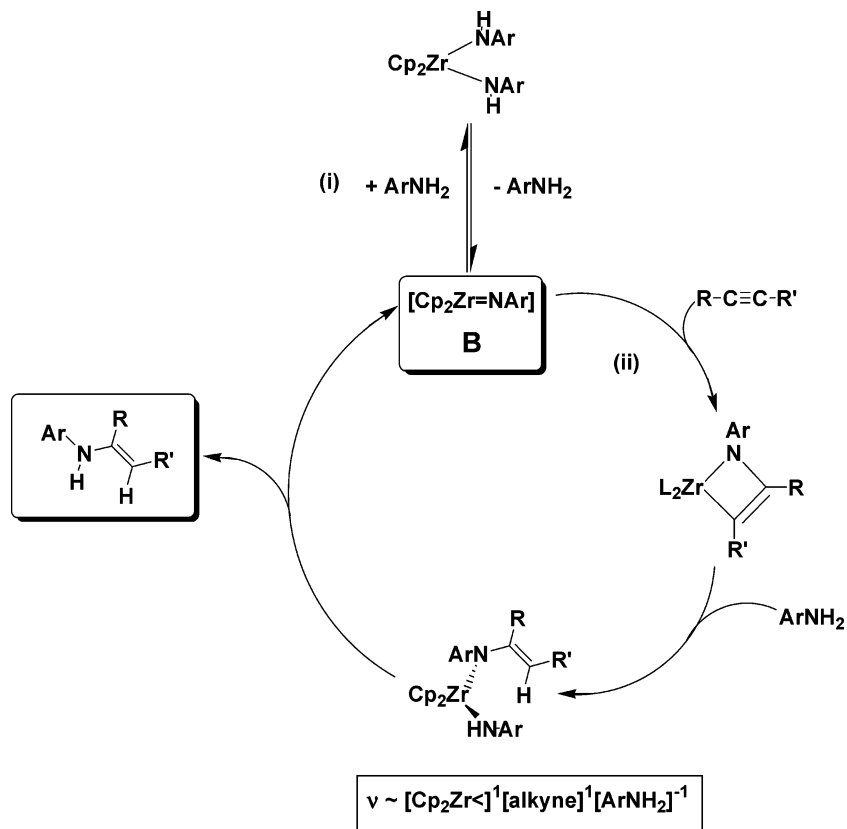
While growing interest in intramolecular aminoalkene<sup>6</sup> and aminoalkyne<sup>7</sup> HA/cyclization mediated by charge-neutral group 4 precatalysts has led to innovative catalyst design, many mechanistic details are not entirely understood. The pathway most often invoked is closely related to that originally proposed

in the pioneering work of Bergman and co-workers (Scheme 2) for *intermolecular* alkyne (and allene) HA with bulky, primary  $ArNH_2$  substrates, mediated by  $Cp_2ZrR_2$  ( $R = Me, N(H)Ar$ ) or  $Cp_2Zr=NAr(THF)$  complexes at elevated temperatures.<sup>8</sup> This pathway involves a rapid pre-equilibrium (step (i), Scheme 2) between  $Cp_2Zr[N(H)Ar]_2$  and  $Cp_2Zr=NAr$  (**B**) +  $H_2NAr$  species, followed by turnover-limiting [2 + 2]  $RC\equiv CR'$  cycloaddition (step (ii), Scheme 2), in agreement with the observed rate law ( $v \sim [Zr]^1 [alkyne]^1 [amine]^{-1}$ ). Similar kinetic studies on  $Cp'_2AnMe_2$ -catalyzed intermolecular addition of bulky and unhindered primary aliphatic amines to terminal alkynes led Eisen and co-workers to propose a similar pathway for  $Cp'_2An <$  catalysts with rapid, irreversible [2 + 2]  $RC\equiv CR'$  cycloaddition.<sup>9</sup> Interestingly, neither  $Cp_2Zr <$  nor

(4) For additional examples of group 3 and lanthanide catalyzed intramolecular HA, see: (a) Bambirra, S.; Tsurugi, H.; van Leusen, D.; Hessen, B. *Dalton Trans.* **2006**, 1157–1161. (b) Gribkov, D. V.; Hultzs, K. C.; Hampel, F. *J. Am. Chem. Soc.* **2006**, *128*, 3748–3759. (c) Panda, T. K.; Zulus, A.; Gamer, M. T.; Roesky, P. W. *Organometallics* **2005**, *24*, 2197–2202. (d) Collin, J.; Daran, J.-C.; Jacquet, O.; Schulz, E.; Trifonov, A. *Chem.—Eur. J.* **2005**, *11*, 3455–3462. (e) Kim, J. Y.; Livinghouse, T. *Org. Lett.* **2005**, *7*, 4391–4393. (f) Kim, J. Y.; Livinghouse, T. *Org. Lett.* **2005**, *7*, 1737–1739. (g) Molander, G. A.; Hasegawa, H. *Heterocycles* **2004**, *64*, 467–474. (h) Lauterwasser, F.; Hayes, P. G.; Brase, S.; Piers, W. E.; Schafer, L. L. *Organometallics* **2004**, *23*, 2234–2237. (i) Hultzs, K. C.; Hampel, F.; Wagner, T. *Organometallics* **2004**, *23*, 2601–2612. (j) O'Shaughnessy, P. N.; Gillespie, K. M.; Knight, P. D.; Munslow, I. J.; Scott, P. *Dalton Trans.* **2004**, 2251–2256. (k) O'Shaughnessy, P. N.; Scott, P. *Tetrahedron: Asymmetry* **2003**, *14*, 1979–1983. (l) O'Shaughnessy, P. N.; Knight, P. D.; Morton, C.; Gillespie, K. M.; Scott, P. *Chem. Commun.* **2003**, 1770–1771. (m) Kim, Y. K.; Livinghouse, T.; Horino, Y. *J. Am. Chem. Soc.* **2003**, *125*, 9560–9561. (n) Molander, G. A.; Pack, S. K. *Tetrahedron* **2003**, *59*, 10581–10591. (o) Molander, G. A.; Pack, S. K. *J. Org. Chem.* **2003**, *68*, 9214–9220. (p) Kim, Y. K.; Livinghouse, T. *Angew. Chem., Int. Ed.* **2002**, *41*, 3645–3647. (q) Bürgstein, M. R.; Berberich, H.; Roesky, P. W. *Chem.—Eur. J.* **2001**, *7*, 3078–3085. (r) Kim, Y. K.; Livinghouse, T.; Bercaw, J. E. *Tetrahedron Lett.* **2001**, *42*, 2933–2935. (s) Molander, G. A.; Dowdy, E. D. *J. Org. Chem.* **1999**, *64*, 6515–6517. (t) Molander, G. A.; Dowdy, E. D. *J. Org. Chem.* **1998**, *63*, 8983–8988.

(5) A slightly modified pathway arguing in favor of turnover-limiting heterocycle protonolysis in intramolecular aminoallene and aminodiene HA/cyclization was proposed from DFT calculations. (a) Tobisch, S. *Chem.—Eur. J.* **2006**, *12*, 2520–2531. (b) Tobisch, S. *J. Am. Chem. Soc.* **2005**, *127*, 11979–11988. (6) (a) Wood, M. C.; Leitch, D. C.; Yeung, C. S.; Kozak, J. A.; Schafer, L. L. *Angew. Chem., Int. Ed.* **2007**, *46*, 354–358. (b) Thomson, R. K.; Bexrud, J. A.; Schafer, L. L. *Organometallics* **2006**, *25*, 4069–4071. (c) Mueller, C.; Loos, C.; Schulenberg, N.; Doye, S. *Eur. J. Org. Chem.* **2006**, 2499–2503. (d) Kim, H.; Lee, P. H.; Livinghouse, T. *Chem. Commun.* **2005**, 5205–5207. (e) Bexrud, J. A.; Beard, J. D.; Leitch, D. C.; Schafer, L. L. *Org. Lett.* **2005**, *7*, 1959–1962. (7) (a) Heutling, A.; Pohlki, F.; Bytschkov, I.; Doye, S. *Angew. Chem., Int. Ed.* **2005**, *44*, 2951–2954. (b) Ackermann, L.; Bergman, R. G.; Loy, R. N. *J. Am. Chem. Soc.* **2003**, *125*, 11956–11963. (c) Li, C.; Thompson, R. K.; Gillon, B.; Patrick, B. O.; Schafer, L. L. *Chem. Commun.* **2003**, 2462–2463. (d) Ackermann, L.; Bergman, R. G. *Org. Lett.* **2002**, *4*, 1475–1478. (e) Bytschkov, I.; Doye, S. *Tetrahedron Lett.* **2002**, *43*, 3715–3718. (f) McGrane, P. L.; Livinghouse, T. *J. Org. Chem.* **1992**, *57*, 1323–1324. (g) McGrane, P. L.; Jensen, M.; Livinghouse, T. *J. Am. Chem. Soc.* **1992**, *114*, 5459–5460. (8) (a) Baranger, A. M.; Walsh, P. J.; Bergman, R. G. *J. Am. Chem. Soc.* **1993**, *115*, 2753–2763. (b) Walsh, P. J.; Baranger, A. M.; Bergman, R. G. *J. Am. Chem. Soc.* **1992**, *114*, 1708–1719.

**Scheme 2.** Proposed [2 + 2] Cycloaddition Mechanistic Pathway Proceeding through a  $\text{Cp}_2\text{Zr}=\text{NAr}$  Intermediate **B** in Intermolecular Alkyne HA with Bulky (Aromatic) Amines<sup>a</sup>



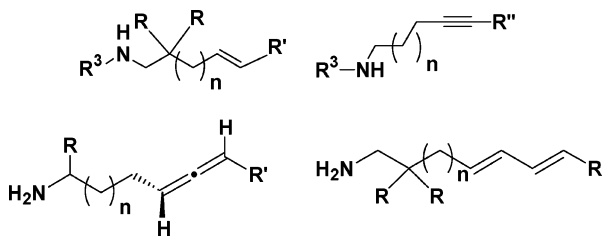
<sup>a</sup> A closely related pathway is proposed for  $\text{Cp}'_2\text{An}$ -catalyzed alkyne HA (see refs 8, 9 and eq 10).

$\text{Cp}'_2\text{An}$  appear to be active catalysts for primary amine additions in less exothermic<sup>1</sup> intermolecular alkene HA.

In contrast to the above findings, more active cationic  $\text{U}(\text{NEt}_2)_3^+\text{BPh}_4^-$  displays kinetic behavior similar to  $\text{Cp}'_2\text{An}$ - and  $\text{Cp}_2\text{Zr}$ -catalyzed intermolecular terminal alkyne HA but effects *secondary*  $\text{HNET}_2$  addition to  $\text{Me}_3\text{SiC}\equiv\text{CH}$ ,<sup>9a</sup> arguing against an  $\text{An}=\text{NR}$  intermediate (vide infra). Moreover, cationic organozirconium and organotitanium complexes effect related *intramolecular* aminoalkene HA/cyclizations, with the reported scope limited *exclusively* to *secondary* aminoalkenes, offering no obvious routes to  $\text{L}_2\text{M}=\text{NR}$  species.<sup>10</sup>

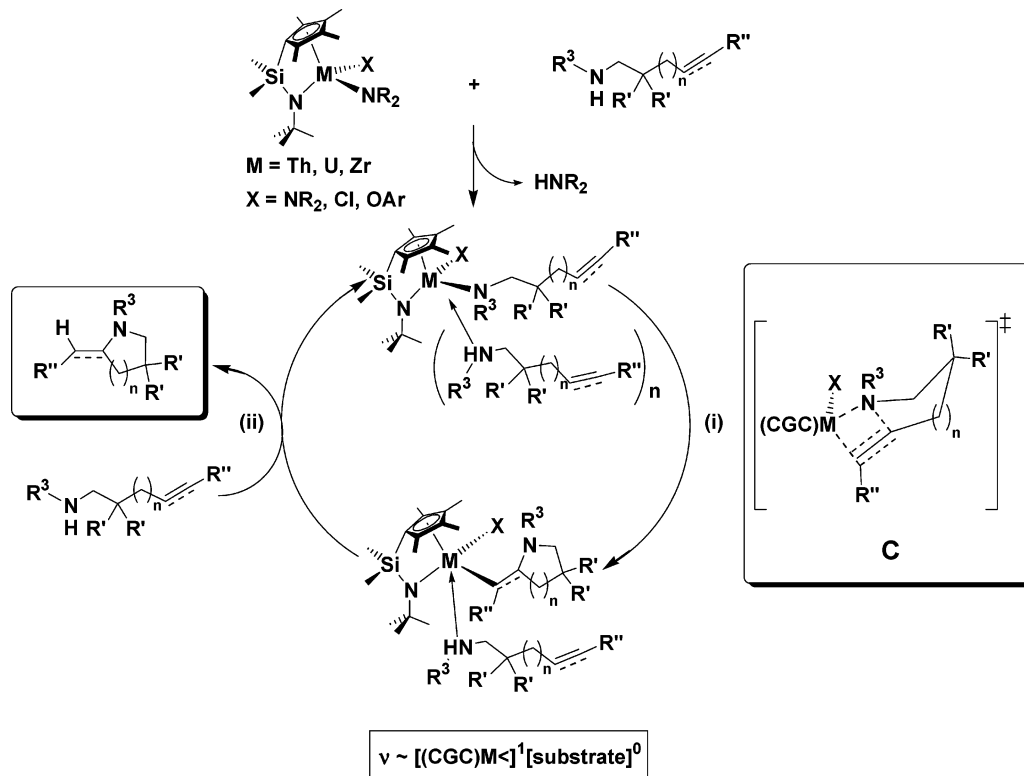
In a companion contribution, we report the rapid and regioselective intramolecular HA/cyclization of primary and secondary amines having diverse tethered C–C unsaturations, mediated by a new series of constrained geometry organoactinide complexes  $(\text{CGC})\text{An}(\text{NMe}_2)_2$  ( $\text{An} = \text{Th}, 1; \text{An} = \text{U}, 2$ ).<sup>11</sup> The scope of C–C unsaturations was explored in depth for terminal and disubstituted alkene, alkyne, allene, and diene substrates, revealing aminoalkene and aminoalkyne turnover frequencies comparable to those of organolanthanide catalysts and exceeding those of organo-group 4 catalysts.<sup>11b</sup> On the basis

of substrate structure–reactivity patterns, kinetic data paralleling organo-4f-element catalysis, and the empirical rate law  $v \sim [(\text{CGC})\text{An}]^1[\text{amine}]^0$ , a “Ln-like” mechanistic scenario proceeding via a tetravalent  $\text{An}-\text{N}(\text{H})\text{R}$   $\sigma$ -bonded species (**C**) was tentatively suggested (Scheme 3). However, while this pathway is plausible for secondary aminoalkenes, cyclizations proceeding through  $\text{An}=\text{NR}$  species cannot a priori be excluded for primary aminoalkenes. These observations along with the paucity of mechanistic information on *intramolecular* HA/cyclization processes mediated by tetravalent group 4 metal centers and known group 4 vs  $\text{An}^{4+}$  M–N bond polarity differences prompted a mechanistic investigation. Herein we report evidence for turnover-limiting  $\text{C}=\text{C}/\text{C}\equiv\text{C}$  insertion at  $\text{An}-\text{N}(\text{H})\text{R}$  species, supported by results with a series of monosubstituted  $(\text{CGC})\text{An}(\text{NR}_2)\text{X}$  complexes ( $\text{X} = \text{nonlabile ligand}$ ) that rapidly and regioselectively mediate intramolecular primary and secondary aminoalkene and aminoalkyne HA/cyclization. Selective substitution of a protonolytically nonlabile  $\text{X}$  ligand for a protonolytically labile amide generates catalysts with only a single nondative  $\sigma$ -bonded substrate moiety, unlikely to support  $\text{An}=\text{NR}$  formation for a comparable energetic cost. Extension to analogous  $(\text{CGC})\text{Zr}$ -catalyzed HA/cyclization



- (9) (a) Wang, J.; Dash, A. K.; Kapon, M.; Berthet, J.-C.; Ephritikhine, M.; Eisen, M. S. *Chem.—Eur. J.* **2002**, *8*, 5384–5396. (b) Straub, T.; Haskel, A.; Neyroud, T. G.; Kapon, M.; Botoshansky, M.; Eisen, M. S. *Organometallics* **2001**, *20*, 5017–5035. (c) Haskel, A.; Straub, T.; Eisen, M. S. *Organometallics* **1996**, *15*, 3773–3775.
- (10) (a) Gribkov, D. V.; Hultsch, K. C. *Angew. Chem., Int. Ed.* **2004**, *43*, 5542–5546. (b) Knight, P. D.; Munslow, I.; O’Shaughnessy, P. N.; Scott, P. *Chem. Commun.* **2004**, 894–895.
- (11) (a) Stubbert, B. D.; Stern, C. L.; Marks, T. J. *Organometallics* **2003**, *22*, 4836–4838. (b) Stubbert, B. D.; Marks, T. J. *J. Am. Chem. Soc.* **2007**, *129*(14), 4253–4271.

**Scheme 3.** Proposed  $\sigma$ -Bond Insertive Mechanism for (CGC)M<sup>-</sup>-Catalyzed Intramolecular HA/Cyclization (M = Zr, Th, U) of Terminal and Disubstituted Aminoalkenes, Aminoalkynes, Aminoallenes, and Aminodienes<sup>a</sup>



<sup>a</sup> When X = NR<sub>2</sub>, two substrate molecules enter the catalytic cycle and two HNR<sub>2</sub> are evolved during precatalyst activation (see ref 11 for additional details regarding the empirical rate law determination).

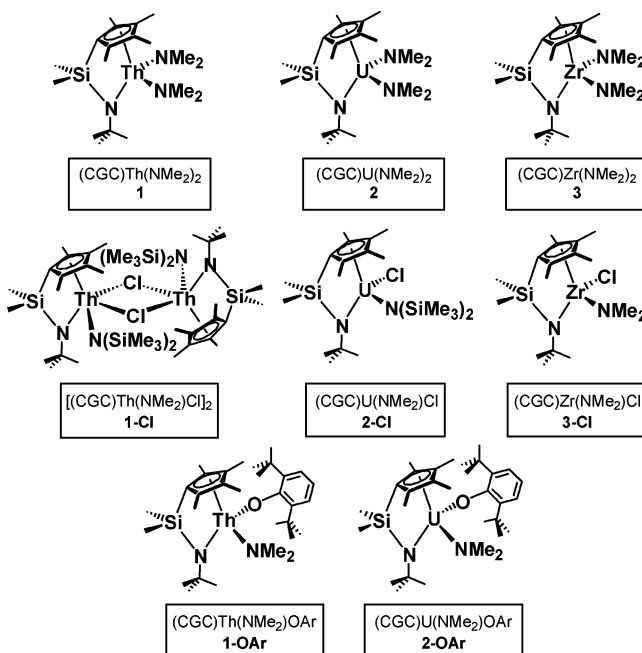
reactions yields similar results. In most cases, the (CGC)M-(NR<sub>2</sub>)X complexes effect HA reactions more rapidly than the corresponding (CGC)MR<sub>2</sub> complexes, further supporting the Scheme 3 pathway.

## Results

In this section we discuss the synthesis and structural characterization of a series of selectively substituted, electrophilic, tetravalent actinide and group 4 (CGC)M(NR<sub>2</sub>)X complexes and mechanistic studies of representative primary and secondary aminoalkene and aminoalkyne intramolecular HA/cyclizations mediated by these complexes. Effects of catalyst substitution, metal ion, and ancillary ligation are presented along with relevant kinetic parameters and deuterium KIE data. It will be seen that these chloride- and aryloxy-substituted complexes are highly active HA/cyclization catalysts that display kinetic and mechanistic signatures inconsistent with M=NR species in the catalytic cycle. A mechanistic pathway proceeding through an M–N  $\sigma$ -bonded species is proposed based on results presented herein.

**Synthesis and Characterization of Chloride- and Aryloxy-Substituted (CGC)M(NR<sub>2</sub>)X Complexes.** (CGC)An-[N(SiMe<sub>3</sub>)<sub>2</sub>]Cl complexes **1-Cl** and **2-Cl** are accessible in excellent yield and high purity from the corresponding AnCl<sub>4</sub> reagents via in situ generation of the tris(hexamethyldisilazido)-actinide chlorides, An[N(SiMe<sub>3</sub>)<sub>2</sub>]<sub>3</sub>Cl,<sup>12</sup> followed by protodeam-

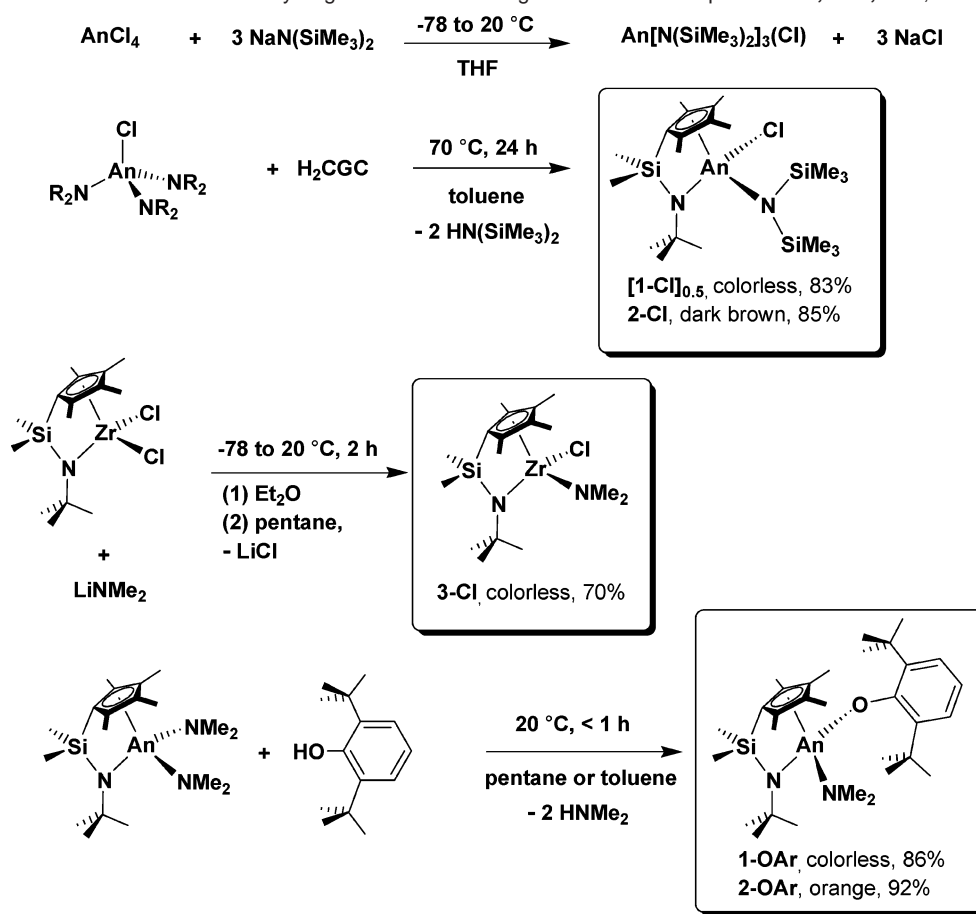
**Chart 1**



ination with diprotic H<sub>2</sub>CGC,<sup>13</sup> evolving hexamethyldisilazane over 16 h at 70 °C (Scheme 4; Chart 1). Owing to unfavorable steric interactions that preclude An[N(SiMe<sub>3</sub>)<sub>2</sub>]<sub>4</sub> formation, the desired complexes are obtained without (CGC)An[N(SiMe<sub>3</sub>)<sub>2</sub>]<sub>2</sub> contamination. The analogous group 4 complex (CGC)Zr-

(12) (a) Simpson, S. J.; Turner, H. W.; Andersen, R. A. *Inorg. Chem.* **1981**, *20*, 2991–2995. (b) Turner, H. W.; Simpson, S. J.; Andersen, R. A. *J. Am. Chem. Soc.* **1979**, *101*, 2782. (c) Turner, H. W.; Andersen, R. A.; Zalkin, A.; Templeton, D. H. *Inorg. Chem.* **1979**, *18*, 1221–1224. (d) Bradley, D. C.; Ghotra, J. S.; Hart, F. A. *Inorg. Nucl. Chem.* **1974**, *10*, 209–211.

(13) Shapiro, P. J.; Schaefer, W. P.; Labinger, J. A.; Bercaw, J. E.; Cotter, W. D. *J. Am. Chem. Soc.* **1994**, *116*, 4623–40.

**Scheme 4.** Syntheses of Constrained Geometry Organoactinide and Organozirconium Complexes **1-Cl**, **2-Cl**, **3-Cl**, **1-OAr**, and **2-OAr**

(NMe<sub>2</sub>)<sub>2</sub>(Cl) **3-Cl** was obtained by traditional salt metathesis from (CGC)ZrCl<sub>2</sub> and LiNMe<sub>2</sub> (Scheme 4; Chart 1). No evidence for amide–halide disproportionation is observed by <sup>1</sup>H NMR spectroscopy at 25 °C over a period of days for any of the chloride-substituted complexes prepared in this study. Solid-state structures were defined by single-crystal X-ray diffraction, indicating that **1-Cl** is a bis( $\mu$ -chloro) dimer in the solid state, while **2-Cl** and **3-Cl** are monomeric (Tables 1 and 2, Figure 1a–c; vide infra).

Aryloxy complexes (CGC)An(NMe<sub>2</sub>)OAr, **1-OAr** and **2-OAr**, are cleanly obtained by protodeamination of (CGC)-An(NMe<sub>2</sub>)<sub>2</sub> complex **1** or **2** with an excess of sterically hindered 2,6-di-*tert*-butylphenol, ArOH (Scheme 4; Chart 1). In the case of An = U, treatment of **2** with 1.8 equiv of ArOH leads to

**Table 1.** Selected Bond Distances (Å) and Angles (deg) for [(CGC)Th[N(SiMe<sub>3</sub>)<sub>2</sub>]( $\mu$ -Cl)]<sub>2</sub> (**1-Cl**), (CGC)U[N(SiMe<sub>3</sub>)<sub>2</sub>]Cl (**2-Cl**), (CGC)Zr(NMe<sub>2</sub>)Cl (**3-Cl**), and (CGC)Th(NMe<sub>2</sub>)OAr (**1-OAr**)<sup>a</sup>

	<b>1-Cl</b>	<b>2-Cl</b>	<b>3-Cl</b>	<b>1-OAr</b>
Cp(cent)–M–N1	91.7	93.1	101.1	90.4
Cp(cent)–M–X	94.8/157.8	108.1	131.9	136.6
Cp(cent)–M–N2	108.8	122.1	104.4	106.9
N1–M–X	107.7(1)	100.52(7)	115.10(7)	115.9(2)
N1–M–N2	110.8(2)	123.8(1)	104.7(1)	102.0(2)
N2–M–X	133.6(1)	106.67(8)	104.06(8)	100.9(2)
Cp(cent)–M	2.53	2.41	2.30	2.55
M–N1	2.335(5)	2.223(3)	2.077(2)	2.293(6)
M–N2	2.334(5)	2.257(3)	2.078(3)	2.252(6)
M–X	2.883(2)/2.964(2)	2.6124(9)	2.437(1)	2.258(5)

<sup>a</sup> See Supporting Information for complete listings (Cp(cent) = Me<sub>4</sub>C ring centroid; X = Cl or OAr).

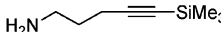
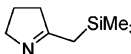
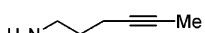
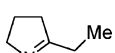
exclusive formation of **2-OAr**, leaving 0.8 equiv of unreacted ArOH. Initial <sup>1</sup>H NMR screening experiments indicate complete consumption of **2** within 30 min of dissolution in benzene-*d*<sub>6</sub> and negligible interaction between the paramagnetic U<sup>4+</sup> ion and unreacted ArOH (as judged by negligible isotropic shifts of the resonances) up to temperatures of 90 °C. Similar experiments carried out with Th complex **1** and 1.2 equiv of ArOH to generate **1-OAr** indicate further reaction and complete consumption of excess ArOH within 60 min at 25 °C. In preparative scale syntheses, the (CGC)Th(OAr)<sub>2</sub> byproduct is easily removed by filtration from concentrated pentane solutions of the otherwise pure monoaryloxy complex. When in situ generated **1-OAr** containing 5–10% (CGC)Th(OAr)<sub>2</sub> is employed in catalytic HA experiments, results are identical to those obtained with isolated **1-OAr**. Complex **1-OAr** was also analyzed via single-crystal X-ray diffraction and shown to be monomeric in the solid state (Tables 1 and 2, Figure 1d).

**Catalytic Intramolecular Hydroamination/Cyclization Experiments.** In this section, results of catalytic intramolecular HA/cyclization of representative aminoalkyne and aminoalkene substrates, mediated by precatalysts (CGC)An(NMe<sub>2</sub>)<sub>2</sub> (An = Th, **1**; An = U, **2**),<sup>11</sup> [(CGC)Th(NR<sub>2</sub>)( $\mu$ -Cl)]<sub>2</sub> (R = SiMe<sub>3</sub>, **1-Cl**),<sup>14</sup> (CGC)M(NR<sub>2</sub>)Cl (M = U, R = SiMe<sub>3</sub>, **2-Cl**; M = Zr, R = Me, **3-Cl**),<sup>14</sup> (CGC)ZrNMe<sub>2</sub> (**3**),<sup>15</sup> (CGC)An(NMe<sub>2</sub>)OAr (OAr = 2,6-di-*tert*-Bu-phenoxide; An = Th, **1-OAr**; An = U,

(14) See Supporting Information for full details.

(15) Carpenetti, D. W.; Kloppenburg, L.; Kupec, J. T.; Petersen, J. L. *Organometallics* **1996**, *15*, 1572–1581.

**Table 2.** Catalytic Data for the Intramolecular HA/Cyclization of Representative Aminoalkyne Substrates **7** and **9** Mediated by the Indicated Actinide and Group 4 Complexes (See Supporting Information for Detailed Reaction Conditions)

Entry	Substrate	Product <sup>a</sup>	Precatalyst <sup>b</sup>	$N_t$ , h <sup>-1</sup> (°C) <sup>c,f</sup>
1.			<b>1</b> , (CGC)Th(NMe <sub>2</sub> ) <sub>2</sub> <sup>d</sup>	82 (25)
2.			<b>1-Cl</b> , [(CGC)Th(NR <sub>2</sub> )Cl] <sub>2</sub>	200 (25)
3.			<b>1-OAr</b> , (CGC)Th(NMe <sub>2</sub> )OAr	37 (25)
4.			<b>2</b> , (CGC)U(NMe <sub>2</sub> ) <sub>2</sub> <sup>d</sup>	3000 (25)
5.			<b>2-Cl</b> , (CGC)U(NR <sub>2</sub> )Cl	280 (25)
6.			<b>2-OAr</b> , (CGC)U(NMe <sub>2</sub> )OAr	52 (25)
7.			<b>4</b> , (Me <sub>2</sub> SiCp'') <sub>2</sub> UBn <sub>2</sub> <sup>d</sup>	10 (60)
8.	<b>7</b>	<b>8</b>	<b>4-Cl</b> , (Me <sub>2</sub> SiCp'') <sub>2</sub> U(Bn)Cl	10 (60)
9.			<b>5</b> , Cp'₂Th(CH₂R) <sub>2</sub> <sup>d</sup>	190 (60)
10.			<b>5-Cl</b> , Cp'₂Th(CH₂R)Cl <sup>e</sup>	1.2 (60)
11.			<b>6</b> , Cp'₂U(CH₂R) <sub>2</sub> <sup>d</sup>	16 (60)
12.			<b>6-Cl</b> , Cp'₂U(CH₂R)Cl <sup>e</sup>	0.4 (60)
13.			<b>3</b> , (CGC)ZrMe <sub>2</sub>	0.2 (60)
14.			<b>3-Cl</b> , (CGC)Zr(NMe <sub>2</sub> )Cl	2.2 (25)
15.			<b>1</b> , (CGC)Th(NMe <sub>2</sub> ) <sub>2</sub> <sup>d</sup>	2.2 (25)
16.			<b>1-Cl</b> , [(CGC)Th(NR <sub>2</sub> )Cl] <sub>2</sub>	7.2 (25)
17.			<b>1-OAr</b> , (CGC)Th(NMe <sub>2</sub> )OAr	0.5 (25)
18.			<b>2</b> , (CGC)U(NMe <sub>2</sub> ) <sub>2</sub> <sup>d</sup>	170 (25)
19.			<b>2-Cl</b> , (CGC)U(NR <sub>2</sub> )Cl	2.9 (25)
20.	<b>9</b>	<b>10</b>	<b>2-OAr</b> , (CGC)U(NMe <sub>2</sub> )OAr	7.2 (25)
21.			<b>3</b> , (CGC)ZrMe <sub>2</sub>	0.2 (60)
22.			<b>3-Cl</b> , (CGC)Zr(NMe <sub>2</sub> )Cl	0.7 (60)

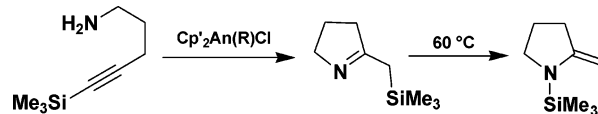
<sup>a</sup> Identified by <sup>1</sup>H NMR spectroscopy and GC/MS. <sup>b</sup> R = SiMe<sub>3</sub>. <sup>c</sup> Determined in situ by <sup>1</sup>H NMR spectroscopy. All yields ≥ 95%. <sup>d</sup> Reference 11b. <sup>e</sup> Isolated product from thermally induced 1,3-sigmatropic shift, *N*-(trimethylsilyl)-2-*exo*-methylene-pyrrolidine (see ref 19). <sup>f</sup> Typical reaction conditions: 2–11 mM [catalyst], 200 mM [aminoalkyne], 5–12 mM Si(*p*-tolyl)<sub>4</sub> internal standard.  $N_t$  determined by least-squares analysis of linear plots of normalized [substrate]/[catalyst] vs time over ≥ 3 $t_{1/2}$ . See Supporting Information for details.

**2-OAr**),<sup>14</sup> Me<sub>2</sub>SiCp''<sub>2</sub>U(CH<sub>2</sub>Ph)<sub>2</sub> (**4**),<sup>16</sup> Me<sub>2</sub>SiCp''<sub>2</sub>U(CH<sub>2</sub>Ph)-Cl (**4-Cl**),<sup>16</sup> Cp'₂An(CH<sub>2</sub>SiMe<sub>3</sub>)<sub>2</sub> (An = Th, **5**; An = U, **6**),<sup>17</sup> and Cp'₂An(CH<sub>2</sub>SiMe<sub>3</sub>)Cl (An = Th, **5-Cl**; An = U, **6-Cl**),<sup>17</sup> are presented. Primary, *N*-unprotected substrates bearing C≡C<sup>11b</sup> and C=C<sup>11b,18</sup> unsaturations are presented first, followed by results with *N*-methyl substituted secondary amine substrates.

**Primary Aminoalkyne Hydroamination.** Intramolecular aminoalkyne HA/cyclization is effectively mediated by bisamido as well as “substituted” chloroamido and aryloxoamido complexes **1–6**. In some cases, the substituted complexes promote **7** → **8** and **9** → **10** cyclizations with far greater catalytic efficiency than the unsubstituted congeners. For example, **7** → **8** conversion mediated by **1-Cl** proceeds at a rate more than double that mediated by **1** at 25 °C ( $N_t$  = 200 h<sup>-1</sup> (**1-Cl**) vs 82 h<sup>-1</sup> (**1**); Table 2, entries 1, 2) and with a 5× greater rate vs

bulkier aryloxo-substituted **1-OAr** ( $N_t$  = 37 h<sup>-1</sup>; Table 2, entry 3). Smaller ionic radius (CGC)U < derivatives display a similar trend, with **2-Cl** mediating **7** → **8** more rapidly than **2-OAr** ( $N_t$  = 280 h<sup>-1</sup> (**2-Cl**) and 52 h<sup>-1</sup> (**2-OAr**) at 25 °C; Table 2, entries 5, 6). This conversion becomes less rapid as ancillary ligation becomes less open, requiring mild heating to achieve moderate  $N_t$  values. Note that no difference in reactivity is observed between unaltered **4** and “substituted” **4-Cl** ( $N_t$  = 10 h<sup>-1</sup> at 60 °C; Table 2, entries 7, 8). More sterically congested Cp'₂An-(R)Cl complexes **5-Cl** and **6-Cl** also mediate this transformation, although catalytic activities are considerably lower than those of their Cp'₂AnR<sub>2</sub> congeners ( $N_t$  = 190 h<sup>-1</sup> (**5**) and 1.2 h<sup>-1</sup> at 60 °C (**5-Cl**);  $N_t$  = 16 h<sup>-1</sup> (**6**) and 0.4 h<sup>-1</sup> (**6-Cl**) at 60 °C; Table 2, entries 9–12).<sup>19</sup> Isolation of volatiles following complete **7** → **8** conversion with **5-Cl** or **6-Cl** and subsequent

(19) Isolated as the *exo*-methylene product from thermally-induced 1,3-sigmatropic shift (–SiMe<sub>3</sub> migration to N; see also ref 3p).



(16) Schnabel, R. C.; Scott, B. L.; Smith, W. H.; Burns, C. J. *J. Organomet. Chem.* **1999**, *591*, 14–23.

(17) Fagan, P. J.; Manriquez, J. M.; Maatta, E. A.; Seyam, A. M.; Marks, T. J. *J. Am. Chem. Soc.* **1981**, *103*, 6650–6667.

(18) (a) Tamaru, Y.; Hojo, M.; Higashimura, H.; Yoshida, Z. *J. Am. Chem. Soc.* **1988**, *110*, 3994–4002. (b) Smith, J. K.; Bergbreiter, D. E.; Newcomb, M. *J. Org. Chem.* **1985**, *50*, 4549–4553.

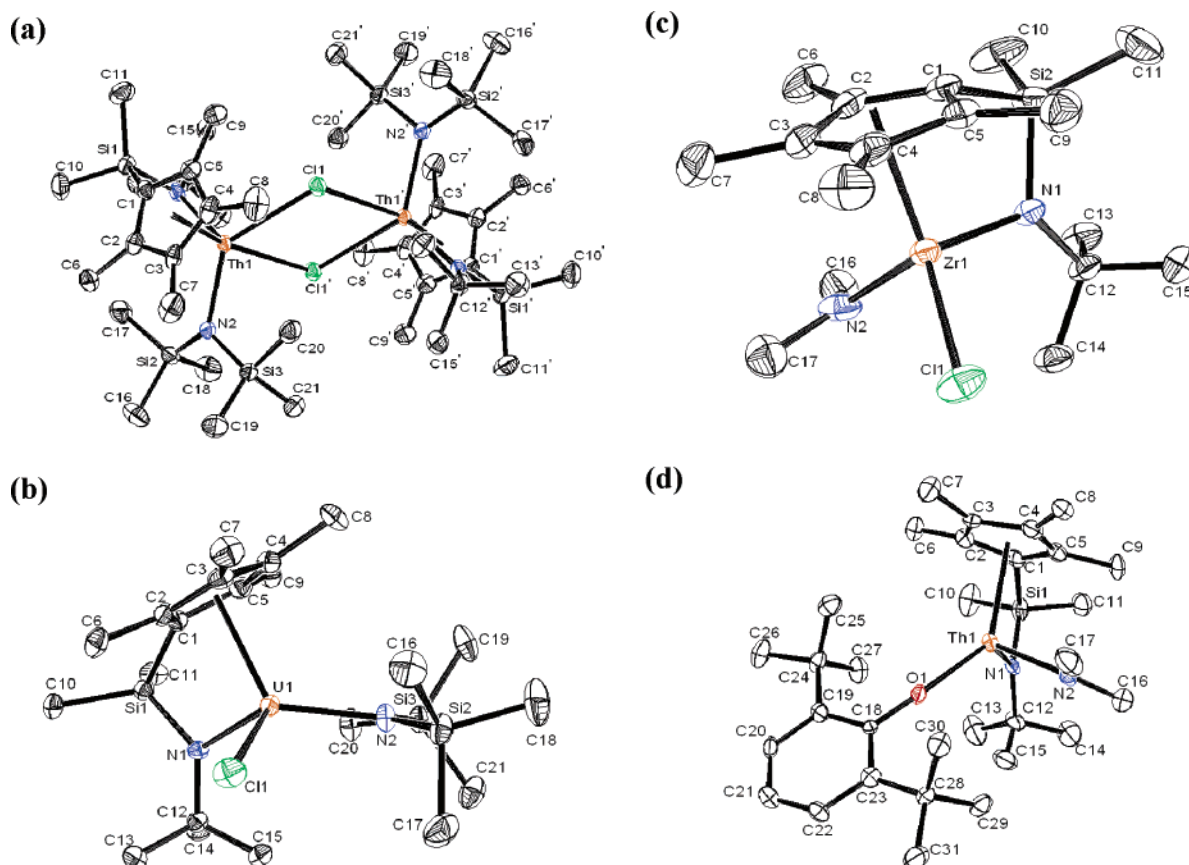


**Figure 1.** ORTEP depictions of solid-state structures of the following precatalysts at  $-120$  °C (a) dimeric  $[(\text{CGC})\text{Th}[\text{N}(\text{SiMe}_3)_2](\mu\text{-Cl})_2]$  (**1-Cl**), (b)  $(\text{CGC})\text{U}[\text{N}(\text{SiMe}_3)_2]\text{Cl}$  (**2-Cl**), (c)  $(\text{CGC})\text{Zr}(\text{NMe}_2)\text{Cl}$  (**3-Cl**), and (d)  $(\text{CGC})\text{Th}(\text{NMe}_2)\text{OAr}$  (**1-OAr**;  $\text{OAr} = 2,6\text{-Bu}_2\text{C}_6\text{H}_3$ ). Thermal ellipsoids are drawn at the 50% probability level. See Table 1, Charts 1–4, and Supporting Information for complete structural data.

GC/MS and  $^1\text{H}$  NMR spectroscopic analyses provide no evidence for formation of free  $\text{HCp}'$  (or its derivatives) during catalytic turnover.

Aminoalkyne transformation  $\mathbf{9} \rightarrow \mathbf{10}$  is also mediated by the present complexes (Table 2). Again, complex **1-Cl** exhibits enhanced activity vs **1** and **1-OAr** ( $N_t = 7.2 \text{ h}^{-1}$  (**1-Cl**) vs  $2.2 \text{ h}^{-1}$  (**1**) and  $0.5 \text{ h}^{-1}$  (**1-OAr**) at  $25$  °C; Table 1, entries 15–17). The  $(\text{CGC})\text{U}$ -catalyzed intramolecular HA/cyclization of **9** is also efficient at  $25$  °C, with efficiencies  $\mathbf{2} > \mathbf{2-OAr} > \mathbf{2-Cl}$  ( $N_t = 170 \text{ h}^{-1}$  (**2**),  $7.2 \text{ h}^{-1}$  (**2-OAr**),  $2.9 \text{ h}^{-1}$  (**2-Cl**); Table 2, entries 18–20). These systems obey the rate law  $\nu \sim [\text{L}_2\text{M}]^{-1}[\text{amine}]^0$  with competitive binding/product inhibition of catalytic turnover sometimes observed at high product concentrations. Eyring and Arrhenius analyses<sup>20</sup> for  $\mathbf{9} \rightarrow \mathbf{10}$  yield  $\Delta H^\ddagger = 16(3) \text{ kcal/mol}$ ,  $\Delta S^\ddagger = -18(9) \text{ eu}$ , and  $E_a = 17(3) \text{ kcal/mol}$  when mediated by **2-Cl** from  $24.9$  °C to  $64.8$  °C with well-behaved kinetics (Figure 2). Furthermore, in situ determination of the solution magnetic moment of **2-Cl** by the Evans' method<sup>21</sup> in benzene- $d_6$  confirms that  $\mu_{\text{eff}}$  for  $(\text{CGC})\text{U}$  complex **2-Cl** prior to activation with substrate **9** is identical to that of the major paramagnetic species present immediately following addition of **9**, as well as during and after complete conversion to **10** under typical HA conditions at  $25$  °C. Note that  $(\text{CGC})\text{MCl}_2$  complexes **1-Cl**<sub>2</sub> ( $\text{M} = \text{Th}$ ),<sup>11</sup> **2-Cl**<sub>2</sub> ( $\text{M} = \text{U}$ ),<sup>11</sup> and **3-Cl**<sub>2</sub> ( $\text{M} = \text{Zr}$ )<sup>15</sup> are *not* active catalysts

for HA/cyclization  $\mathbf{9} \rightarrow \mathbf{10}$  at  $25$  °C ( $\text{M} = \text{Th}$ ,  $\text{U}$ ) or  $60$  °C ( $\text{M} = \text{Zr}$ ) in  $\text{C}_6\text{D}_6$ .

Intramolecular aminoalkyne HA/cyclizations  $\mathbf{7} \rightarrow \mathbf{8}$  and  $\mathbf{9} \rightarrow \mathbf{10}$  are efficient when catalyzed by  $(\text{CGC})\text{Zr}$  complexes **3** and **3-Cl**, although moderate heating is required to obtain activities comparable to the larger  $(\text{CGC})\text{An}$  complexes (Table 2). More reactive  $\text{Me}_3\text{Si}$ -substituted **7** is converted to exocyclic imine **8** with a markedly enhanced rate (ca.  $100 \times$ ) when mediated by **3-Cl** vs **3** ( $N_t = 2.2 \text{ h}^{-1}$  at  $25$  °C (**3-Cl**) vs  $0.2 \text{ h}^{-1}$  at  $60$  °C (**3**); Table 2, entries 13, 14). Catalytic conversion of  $\text{Me}$ -substituted aminoalkyne **9** proceeds with a similar although less pronounced **3-Cl** vs **3** rate effect; i.e., a ca.  $3 \times$  increase in activity is observed for **3-Cl** ( $N_t = 0.7 \text{ h}^{-1}$  (**3-Cl**) vs  $0.2 \text{ h}^{-1}$  (**3**) at  $60$  °C; Table 2, entries 21, 22). These systems also obey the rate law  $\nu \sim [\text{L}_2\text{M}]^{-1}[\text{amine}]^0$  with competitive binding/product inhibition of catalytic turnover sometimes observed at high [product]. Eyring and Arrhenius analyses<sup>20</sup> for  $\mathbf{7} \rightarrow \mathbf{8}$  mediated by **3-Cl** provide direct comparison to  $\text{L}_2\text{An}$  and  $\text{L}_2\text{-Ln}$  catalysts, affording  $\Delta H^\ddagger = 11(2) \text{ kcal/mol}$ ,  $\Delta S^\ddagger = -35(7) \text{ eu}$ , and  $E_a = 12(2) \text{ kcal/mol}$  from  $24.8$  °C to  $67.3$  °C displaying well-behaved kinetics (Figure 3).

**Primary Aminoalkene Hydroamination.** Intramolecular aminoalkene HA/cyclization of representative substrate **11** is effectively mediated by both “substituted” and unsubstituted bisamido complexes **1–3**. Comparison between Th complexes shows decreased activity for **1-Cl** vs **1** at  $25$  °C ( $N_t = 3.3 \text{ h}^{-1}$  (**1-Cl**) vs  $15 \text{ h}^{-1}$  (**1**); Table 3, entries 1, 2), although dimeric

(20) Espenson, J. H. *Chemical Kinetics and Reaction Mechanisms*, 2nd ed.; McGraw-Hill, Inc.: New York, 1995.

(21) (a) Schubert, E. M. *J. Chem. Educ.* **1992**, *69*, 62. (b) Evans, D. F. *J. Chem. Soc.* **1959**, 2003–2005.

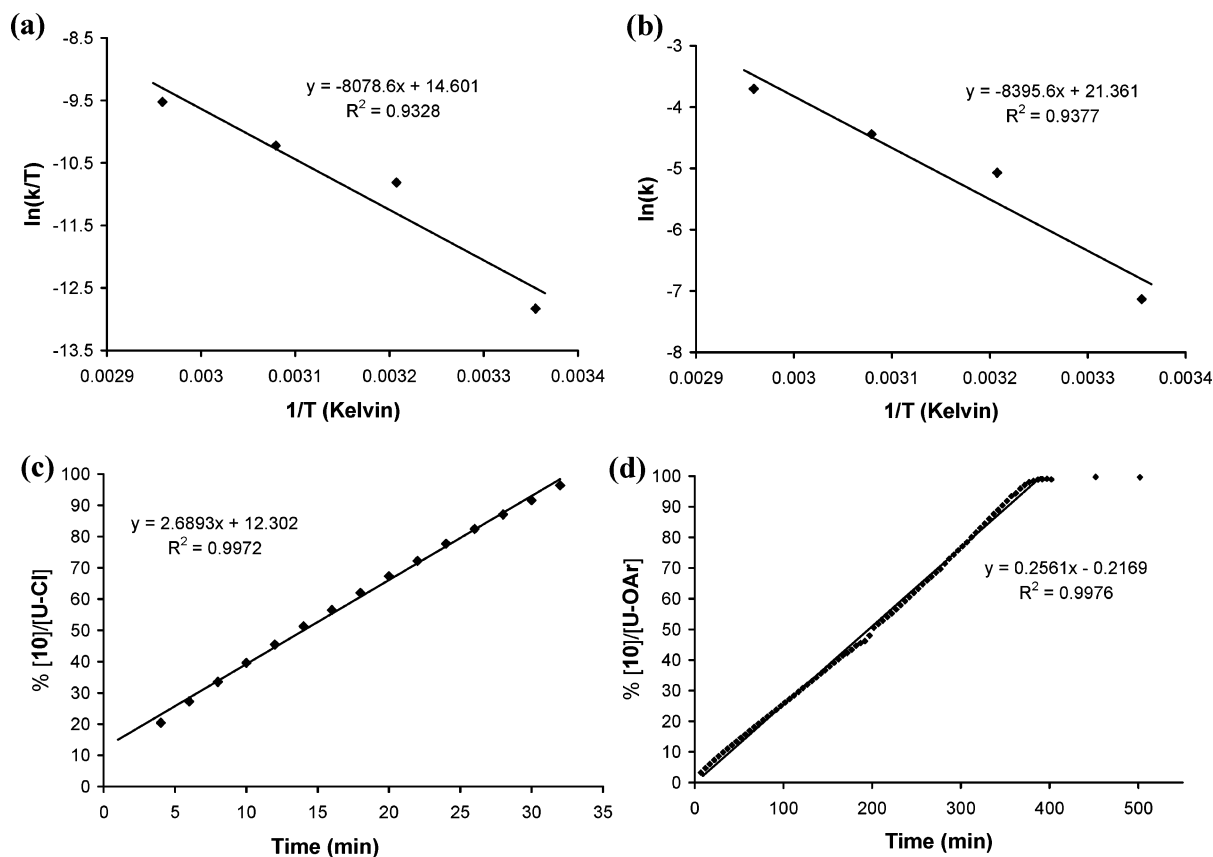


**Figure 2.** (a) Eyring plot for conversion **9**  $\rightarrow$  **10** catalyzed by (CGC)U[N(SiMe<sub>3</sub>)<sub>2</sub>]Cl (**2-Cl**) from 24.9 to 64.8 °C in C<sub>6</sub>D<sub>6</sub> ( $\Delta H^\ddagger = 16(3)$  kcal/mol,  $\Delta S^\ddagger = -18(9)$  eu). (b) Arrhenius plot for conversion **9**  $\rightarrow$  **10** catalyzed by **2-Cl** over a 40 °C range in C<sub>6</sub>D<sub>6</sub> ( $E_a = 17(3)$  kcal/mol). (c) Representative kinetic plot for conversion **9**  $\rightarrow$  **10** catalyzed by **2-Cl** in C<sub>6</sub>D<sub>6</sub> at 40 °C. (d) Representative kinetic plot for conversion **9**  $\rightarrow$  **10** catalyzed by (CGC)U(NMe<sub>2</sub>)OAr (**2-OAr**) at 25 °C in C<sub>6</sub>D<sub>6</sub>.  $N_t$  (and rate constants) determined by least-squares analysis of linear plots of normalized [substrate]/[catalyst] vs time over  $\geq 3t_{1/2}$ . Standard reaction conditions were employed in all catalytic reactions. Deviation from linearity at high conversion is attributed to product inhibition. See the Supporting Information and ref 11b for details.

**1-Cl** may remain intact and, therefore, sterically encumbered during catalysis. Precatalyst **1-Cl'**, generated by treatment of **1-Cl** with (noncyclizable) neopentylamine at 25 °C in C<sub>6</sub>D<sub>6</sub> for 24 h followed by removal of byproduct HN(SiMe<sub>3</sub>)<sub>2</sub>, exhibits an identical  $N_t$  (vs **1-Cl**) for cyclization **11**  $\rightarrow$  **12** at 25 °C, suggesting that the structure of **1-Cl** in solution (monomer vs dimer) does not change with a large amine excess. Aryloxide-substituted **1-OAr** and **2-OAr** exhibit diminished reactivity with moderate  $N_t$  at 60 °C (0.6 h<sup>-1</sup> and 1.5 h<sup>-1</sup>, respectively; Table 3, entries 3, 6). Interestingly, complex **2-Cl** promotes **11**  $\rightarrow$  **12** cyclization with  $>2\times$  the catalytic efficiency of **2** at 25 °C ( $N_t = 6.2$  h<sup>-1</sup> vs 2.5 h<sup>-1</sup>; Table 3, entries 4, 5). This **2/2-Cl** trend maintains for **11-d<sub>2</sub>**  $\rightarrow$  **12-d<sub>2</sub>**, where deuterium KIEs are significant at 25 °C, with  $k_H/k_D = 3.3(5)$  and 2.6(4), respectively ( $N_t = 0.8$  h<sup>-1</sup> (**2**) and 2.4 h<sup>-1</sup> (**2-Cl**) at 25 °C). Likewise, organozirconium complex **3-Cl** exhibits greater catalytic activity than **3**, although rates are considerably more sluggish than that for the Th analogue ( $N_t = 0.14$  h<sup>-1</sup> (**3-Cl**) vs 0.07 h<sup>-1</sup> (**3**); Table 3, entries 7, 8). Although the (CGC)Zr< complexes exhibit sluggish cyclization rates and require elevated reaction temperatures, no reactions other than precatalyst protonolysis and CH<sub>4</sub>/HNMe<sub>2</sub> evolution are observed by <sup>1</sup>H NMR spectroscopy below 100 °C. Furthermore, neither (CGC)Zr<-mediated reaction evidences an induction period consistent with a disproportionation or equilibration process preceding catalytic turnover (vide infra). These systems obey the rate law  $\nu \sim [L_2M<]^{-1}[\text{amine}]^0$  with competitive binding/product inhibition of catalytic turnover

sometimes observed at high [product]. Eyring and Arrhenius analyses<sup>20</sup> for **11**  $\rightarrow$  **12** yield  $\Delta H^\ddagger = 10(3)$  kcal/mol,  $\Delta S^\ddagger = -43(9)$  eu, and  $E_a = 11(3)$  kcal/mol when mediated by **2-OAr** from 63 °C to 100 °C (Figure 4) with well-behaved kinetics.

**Secondary Aminoalkene and Aminoalkyne Hydroamination.** Intramolecular aminoalkene and aminoalkyne HA/cyclization of representative secondary amines **13** and **15** is effectively mediated by unsubstituted and “substituted” complexes **1–3** and **1–3**, **5–6**, respectively. Chloride-substituted **3-Cl** mediates *N*-methylaminoalkene cyclization **13**  $\rightarrow$  **14** significantly more rapidly than **3**, although considerably more sluggishly than the more reactive chloride-substituted organoactinide complexes ( $N_t = 0.1$  h<sup>-1</sup> (**1-Cl**) and 0.2 h<sup>-1</sup> (**2-Cl**) at 60 °C vs 0.4 h<sup>-1</sup> (**3-Cl**) at 90 °C and 0.2 h<sup>-1</sup> (**3**) at 120 °C; Table 4, entries 2, 5, 7–8). Cyclization **13**  $\rightarrow$  **14** catalyzed by **1-OAr** or **2-OAr** proceeds more sluggishly, with comparable efficiencies observed at 120 °C (0.5 h<sup>-1</sup>; Table 4, entries 3, 6). Mediated by **1** or **2** in the more polar 1:1 *ortho*-C<sub>6</sub>H<sub>4</sub>F<sub>2</sub>/C<sub>6</sub>D<sub>6</sub> solvent mixture, this transformation proceeds with considerably diminished catalytic efficiency ( $>10\times$  for **2**), although catalyst decomposition via F<sup>-</sup> abstraction may occur for **1** (An = Th).<sup>22</sup> Note that  $N_t$  values for **13**  $\rightarrow$  **14** differ little between the **1**- and **2**-catalyzed processes and those catalyzed by the corresponding monochloro derivatives (Table 4, entries 1–2, 4–5). As noted above, these systems

(22) Heating (CGC)Th(NMe<sub>2</sub>)<sub>2</sub> in a 1:1 *ortho*-C<sub>6</sub>H<sub>4</sub>F<sub>2</sub>/C<sub>6</sub>D<sub>6</sub> solvent mixture to 60 °C in the absence of substrate leads to rapid decomposition of **1** and formation of an uncharacterized product.



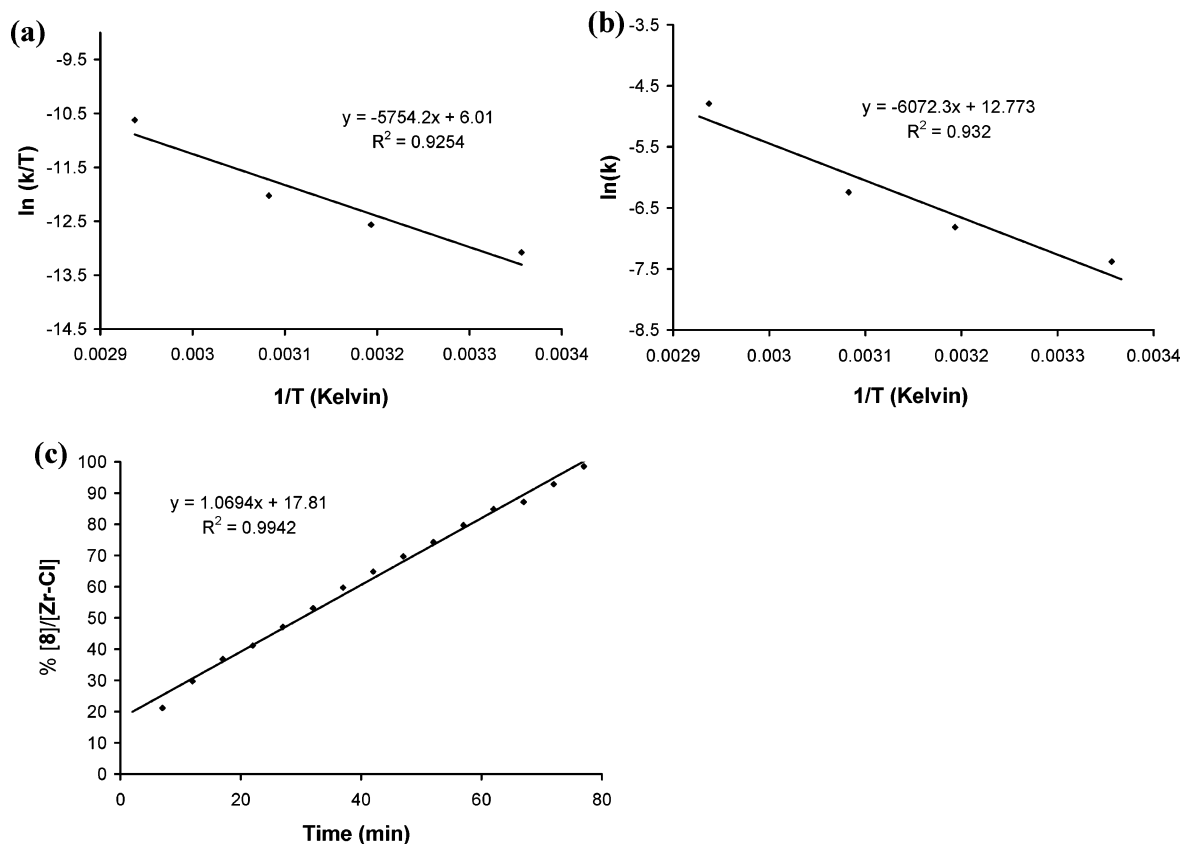


**Figure 3.** (a) Eyring plot for conversion **7**  $\rightarrow$  **8** catalyzed by (CGC)Zr(NMe<sub>2</sub>)Cl (**3-Cl**) from 24.8 °C to 67.3 °C in C<sub>6</sub>D<sub>6</sub> ( $\Delta H^\ddagger = 11(2)$  kcal/mol,  $\Delta S^\ddagger = -35(7)$  eu). (b) Arrhenius plot for **7**  $\rightarrow$  **8** conversion catalyzed by **3-Cl** over 42 °C in C<sub>6</sub>D<sub>6</sub> ( $E_a = 12(2)$  kcal/mol). (c) Representative kinetic plot for conversion **7**  $\rightarrow$  **8** catalyzed by **3-Cl** in C<sub>6</sub>D<sub>6</sub> at 25 °C.  $N_t$  (and rate constants) determined by least-squares analysis of linear plots of normalized [substrate]/[catalyst] vs time over  $\geq 3t_{1/2}$ . Standard reaction conditions were employed in all catalytic reactions. Deviation from linearity at high conversion is attributed to product inhibition. See the Supporting Information for details.

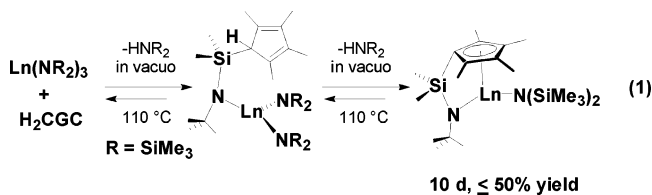
also obey the rate law  $v \sim [L_2M<]^{1/2}[amine]^0$  with competitive binding/product inhibition of catalytic turnover sometimes observed at high [product]. Eyring and Arrhenius analyses<sup>20</sup> for **13**  $\rightarrow$  **14** yield  $\Delta H^\ddagger = 9(3)$  kcal/mol,  $\Delta S^\ddagger = -48(6)$  eu, and  $E_a = 10(3)$  kcal/mol when mediated by **1** from 60 °C to 110 °C (Figure 4) with well-behaved kinetics.

*N*-methylaminoalkyne **15** is also converted to exocyclic pyrrolidine **16** by (CGC)An<, (CGC)Zr<, and Cp'<sub>2</sub>An< complexes, although with considerably less efficiency when promoted by **3** ( $N_t = 80$  h<sup>-1</sup> (**1**) and 120 h<sup>-1</sup> (**2**) at 25 °C, vs  $N_t = 0.3$  h<sup>-1</sup> (**3**) at 90 °C; Table 4, entries 9, 11, 13). Metallocenes **5** and **6** are also effective precatalysts for this cyclization, with intermediate efficiencies far less than those for **1** and **2** but considerably greater than that for **3** ( $N_t = 7.4$  h<sup>-1</sup> (**5**) and 15 h<sup>-1</sup> (**6**) at 90 °C; Table 4, entries 15, 16). Monoamidochloride complexes **1–3** also mediate **15**  $\rightarrow$  **16** conversion effectively, although with marked reduction in efficiency ( $N_t = 24$  h<sup>-1</sup> (**1-Cl**) and 33 h<sup>-1</sup> (**2-Cl**) at 60 °C, and 0.02 h<sup>-1</sup> at 90 °C (**3-Cl**); Table 4, entries 10, 12, 14).

## Discussion

In this section, the synthesis, structural characterization, and hydroamination/cyclization catalytic characteristics of bisamido and substituted, monoamido complexes **1–6** are first discussed. Implications of these findings are then presented in the context of plausible mechanistic pathways for actinide vs group 4 mediated intramolecular aminoalkene and aminoalkyne HA/cyclizations.

**Synthesis and Characterization of Monosubstituted (CGC)M(NR<sub>2</sub>)X Complexes.** Monosubstituted chloride and aryloxo complexes **1–3** are obtained in excellent yield and purity in a single step from known reagents (Scheme 4). Neutral, monomeric tris(amido)actinide chlorides, An[N(SiMe<sub>3</sub>)<sub>2</sub>]<sub>3</sub>Cl,<sup>12</sup> are obtained quantitatively in toluene without competing formation of tris(amido)actinide hydrides<sup>12a,b</sup> or of potentially inhibitory, charged/solvated byproducts. Treatment in situ with H<sub>2</sub>CGC<sup>13</sup> cleanly affords chloroamido complexes **1-Cl** and **2-Cl** in up to 85% isolated yield. Note that the enhanced Lewis acidity of An[N(SiMe<sub>3</sub>)<sub>2</sub>]<sub>3</sub>Cl vs homoleptic Ln[N(SiMe<sub>3</sub>)<sub>2</sub>]<sub>3</sub> complexes (used in the synthesis of closely related (CGC)Ln–N(SiMe<sub>3</sub>)<sub>2</sub> complexes; eq 1)<sup>3k</sup> leads to significant rate enhancements in **1-Cl** and **2-Cl** generation, requiring markedly lower reaction temperatures and proceeding without periodic removal of evolved HN(SiMe<sub>3</sub>)<sub>2</sub> (Scheme 4). <sup>1</sup>H NMR spectra of **1-Cl** and **2-Cl** recorded in noncoordinating solvents at 20–80 °C are consistent with C<sub>1</sub> symmetry in solution and evidence no detectable ligand redistribution or dynamic equilibria on the NMR time scale.



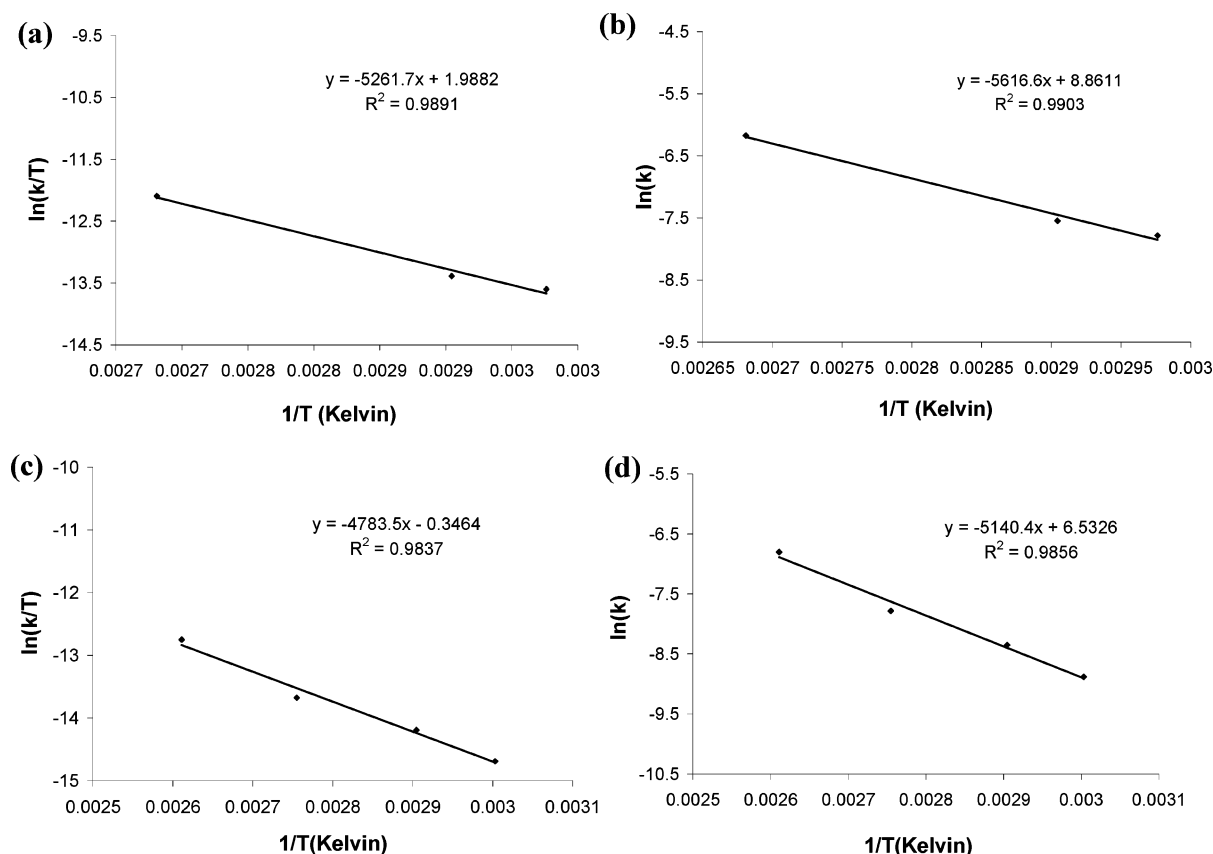


**Figure 4.** (a) Eyring plot for conversion **11**  $\rightarrow$  **12** catalyzed by (CGC)U(NMe<sub>2</sub>)OAr (**2-OAr**) from 63 to 100 °C in C<sub>6</sub>D<sub>6</sub> ( $\Delta H^\ddagger = 10(3)$  kcal/mol,  $\Delta S^\ddagger = -43(9)$  eu). (b) Arrhenius plot for conversion **11**  $\rightarrow$  **12** catalyzed by **2-OAr** over a 40 °C range in C<sub>6</sub>D<sub>6</sub> ( $E_a = 11(3)$  kcal/mol). (c) Eyring plot for conversion **13**  $\rightarrow$  **14** catalyzed by (CGC)Th(NMe<sub>2</sub>)<sub>2</sub> (**1**) from 60 to 110 °C in C<sub>6</sub>D<sub>6</sub> ( $\Delta H^\ddagger = 9(3)$  kcal/mol,  $\Delta S^\ddagger = -48(6)$  eu). (d) Arrhenius plot for conversion **13**  $\rightarrow$  **14** catalyzed by **1** over a 50 °C range in C<sub>6</sub>D<sub>6</sub> ( $E_a = 10(3)$  kcal/mol).  $N_t$  and rate constants determined by least-squares analysis of linear plots of normalized [substrate]/[catalyst] vs time over  $\geq 3t_{1/2}$ . Standard reaction conditions were employed in all catalytic reactions. See the Supporting Information and ref 11b for details.

**Table 3.** Catalytic Data for the Intramolecular HA/Cyclization **11**  $\rightarrow$  **12** Mediated by the Indicated Actinide and Group 4 Complexes (See Supporting Information for Reaction Conditions)

Entry	Substrate	Product <sup>a</sup>	Precatalyst <sup>b</sup>	$N_t$ , h <sup>-1</sup> (°C) <sup>c,e</sup>
1.			<b>1</b> , (CGC)Th(NMe <sub>2</sub> ) <sub>2</sub> <sup>d</sup>	15 (25)
2.			<b>1-Cl</b> , [(CGC)Th(NR <sub>2</sub> )Cl] <sub>2</sub>	3.3 (25)
3.			<b>1-OAr</b> , (CGC)Th(NMe <sub>2</sub> )OAr	0.6 (60)
4.			<b>2</b> , (CGC)U(NMe <sub>2</sub> ) <sub>2</sub> <sup>d</sup>	2.5 (25)
5.	<b>11</b>	<b>12</b>	<b>2-Cl</b> , (CGC)U(NR <sub>2</sub> )Cl	6.2 (25)
6.			<b>2-OAr</b> , (CGC)U(NMe <sub>2</sub> )OAr	1.5 (60)
7.			<b>3</b> , (CGC)ZrMe <sub>2</sub>	0.07 (100)
8.			<b>3-Cl</b> , (CGC)Zr(NMe <sub>2</sub> )Cl	0.14 (100)

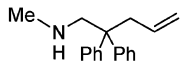
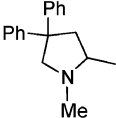
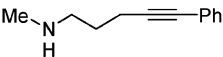
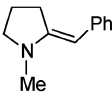
<sup>a</sup> Identified by <sup>1</sup>H NMR spectroscopy and GC/MS. <sup>b</sup> R = SiMe<sub>3</sub>. <sup>c</sup> Determined in situ by <sup>1</sup>H NMR spectroscopy. All yields > 95%. <sup>d</sup> Reference 11b. <sup>e</sup> Typical reaction conditions: 2–11 mM [catalyst], 200 mM [aminoalkene], 5–12 mM Si(p-tolyl)<sub>4</sub> internal standard.  $N_t$  determined by least-squares analysis of linear plots of normalized [substrate]/[catalyst] vs time over  $\geq 3t_{1/2}$ . See Supporting Information for details.

Furthermore, the known insolubility of (CGC)AnCl<sub>2</sub> complexes in low-polarity solvents<sup>11</sup> and absence of **1-Cl**/**2-Cl**-derived precipitates over several days in C<sub>6</sub>D<sub>6</sub> suggest that the bulky -N(SiMe<sub>3</sub>)<sub>2</sub> moiety affords sufficient kinetic stabilization to prevent halide/amide redistribution.

Interestingly, subtle An<sup>4+</sup> ionic radius differences (nine-coordinate: Th<sup>4+</sup> 1.09 Å vs U<sup>4+</sup> 1.05 Å)<sup>23</sup> apparently result in Th complex **1-Cl** crystallizing as a C<sub>2</sub>-symmetric bis( $\mu$ -chloro) dimer (Figure 1a). Single crystals of **1-Cl** (Table S1) contain planar, diamond-shaped Th<sub>2</sub>( $\mu$ -Cl)<sub>2</sub> cores with Th–Cl–Th' and Cl–Th–Cl' angles of 113.66(5)° and 66.34(5)°, respectively, and a large Th·····Th distance of 4.89(1) Å. The Cp(centroid)–

(23) Shannon, R. D. *Acta Crystallogr.* **1976**, *A32*, 751–67.

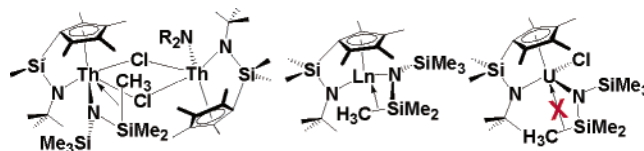
**Table 4.** Catalytic Data for the Intramolecular HA/Cyclization of Representative Secondary Aminoalkene **13** and Secondary Aminoalkyne **15** Mediated by the Indicated Actinide and Group 4 Complexes (See Supporting Information for Reaction Conditions)

Entry	Substrate	Product <sup>a</sup>	Precatalyst <sup>b</sup>	$N_t$ , h <sup>-1</sup> (°C) <sup>c,e</sup>
1.			<b>1</b> , (CGC)Th(NMe <sub>2</sub> ) <sub>2</sub> <sup>d</sup>	0.5 (60)
2.			<b>1-Cl</b> , [(CGC)Th(NR <sub>2</sub> )Cl] <sub>2</sub>	0.1 (60)
3.			<b>1-OAr</b> , (CGC)Th(NMe <sub>2</sub> )OAr	0.5 (120)
4.			<b>2</b> , (CGC)U(NMe <sub>2</sub> ) <sub>2</sub> <sup>d</sup>	0.9 (60)
5.			<b>2-Cl</b> , (CGC)U(NR <sub>2</sub> )Cl	0.2 (60)
6.			<b>2-OAr</b> , (CGC)U(NMe <sub>2</sub> )OAr	0.5 (120)
7.			<b>3</b> , (CGC)ZrMe <sub>2</sub>	0.2 (120)
8.			<b>3-Cl</b> , (CGC)Zr(NMe <sub>2</sub> )Cl	0.4 (90)
-----				
9.			<b>1</b> , (CGC)Th(NMe <sub>2</sub> ) <sub>2</sub> <sup>d</sup>	80 (25)
10.			<b>1-Cl</b> , [(CGC)Th(NR <sub>2</sub> )Cl] <sub>2</sub>	24 (60)
11.			<b>2</b> , (CGC)U(NMe <sub>2</sub> ) <sub>2</sub> <sup>d</sup>	120 (25)
12.			<b>2-Cl</b> , (CGC)U(NR <sub>2</sub> )Cl	33 (25)
13.			<b>3</b> , (CGC)ZrMe <sub>2</sub>	0.3 (90)
14.			<b>3-Cl</b> , (CGC)Zr(NMe <sub>2</sub> )Cl	0.02 (90)
15.			<b>5</b> , Cp' <sub>2</sub> Th[CH <sub>2</sub> (SiMe <sub>3</sub> ) <sub>2</sub> ]	7.4 (60)
16.	<b>6</b> , Cp' <sub>2</sub> U[CH <sub>2</sub> (SiMe <sub>3</sub> ) <sub>2</sub> ]	15 (60)		

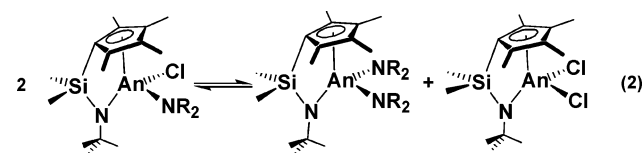
<sup>a</sup> Identified by <sup>1</sup>H NMR spectroscopy and GC/MS. <sup>b</sup> R = SiMe<sub>3</sub>. <sup>c</sup> Determined in situ by <sup>1</sup>H NMR spectroscopy. All yields  $\geq$  95%. <sup>d</sup> Reference 11b. <sup>e</sup> Typical reaction conditions: 2–11 mM [catalyst], 200 mM [substrate], 5–12 mM Si(*p*-tolyl)<sub>4</sub> internal standard.  $N_t$  determined by least-squares analysis of linear plots of normalized [substrate]/[catalyst] vs time over  $\geq 3t_{1/2}$ . See Supporting Information for details.

Th–N(Bu) angle of 91.7° compares well with that in **1** (91.3°)<sup>11</sup> and **1-OAr** (90.4°; vide infra), indicating significant steric openness (Chart 2).<sup>11,24</sup> The 2.334(5) Å Th–N(SiMe<sub>3</sub>)<sub>2</sub> bond distance in **1-Cl** is considerably longer than the 2.27(1) Å and 2.252(6) Å Th–NMe<sub>2</sub> distances in **1** (average) and **1-OAr**, respectively, but statistically comparable ( $<3\sigma$ ) to Th–N(Bu) distances in **1-Cl** (2.335(5) Å), **1** (2.315(4) Å), and **1-OAr** (2.293(6) Å), reflecting the electron-withdrawing capacity of the –SiMe<sub>3</sub> groups.<sup>25</sup> Bridging Th–Cl distances of 2.883(2) Å and 2.964(2) Å in **1-Cl** are quite similar to those of 2.874(2) Å and 2.933(2) Å in [(CGC)Th( $\mu$ -Cl)<sub>2</sub>-(Cl)Li(OEt)<sub>2</sub>]<sub>2</sub>.<sup>24a</sup> The similar U<sup>4+</sup> dimer [(N[CH<sub>2</sub>CH<sub>2</sub>N-(SiMe<sub>3</sub>)<sub>3</sub>]<sub>3</sub>U( $\mu$ -Cl)<sub>2</sub>] also displays a planar U<sub>2</sub>( $\mu$ -Cl)<sub>2</sub> diamond core with U–Cl–U' and Cl–U–Cl' angles of 104.51(9)° and 75.49(8)°, respectively (Chart 2).<sup>24c</sup> Monomeric N[CH<sub>2</sub>CH<sub>2</sub>N-(SiMe<sub>3</sub>)<sub>3</sub>]UCl possesses a terminal U–Cl distance of 2.641(5) Å, roughly 10% shorter than that in the corresponding dimer.<sup>24b</sup> The solid-state structures (Table S1) of monomeric **2-Cl** (Figure 1b) and **3-Cl** (Figure 1c) also display steric openness nearly identical to that in unsubstituted analogues **2** and **3**. Cp(centroid)–M–N(Bu) angles of 91.7° (**1-Cl**), 93.1° (**2-Cl**), and 101.1° (**3-Cl**) correlate with the metal ionic radius,<sup>23</sup> evidencing greater coordinative unsaturation with

increasing ion size. Also, note the comparatively short Th···C(20) distance of 3.18(1) Å in **1-Cl** vs U···C(20) of 3.53(1) Å in **2-Cl**, suggesting agostic Si–C( $\alpha$ ) bond stabilization in the larger Th complex.<sup>3k,26,27</sup>



Redistribution processes analogous to eq 2 are known to occur, especially in complexes with larger actinide ions in open ligation environments and in the absence of coordinating Lewis bases.<sup>26,28</sup> To probe the importance of complicating



(CGC)M(NR<sub>2</sub>)Cl redistribution processes during catalytic reactions, aryloxy-substituted precatalysts **1-OAr** and **2-OAr** were generated via protodeamination of **1** and **2** with ArOH (2,6-di-*t*-Bu-phenol; Scheme 4). The disparity in An<sup>4+</sup> ionic radii/covalency is evident where organouranium complex **2-OAr** does not undergo reaction with excess phenol up to 90 °C, whereas organothorium complex **1-OAr** rapidly forms (CGC)Th(OAr)<sub>2</sub> at 25 °C. In situ generated precatalysts **1-OAr** and **2-OAr**

(24) (a) Golden, J. T.; Kazul'kin, D. N.; Scott, B. L.; Voskoboinikov, A. Z.; Burns, C. J. *Organometallics* **2003**, *22*, 3971–3973. (b) Roussel, P.; Alcock, N. W.; Boaretto, R.; Kingsley, A. J.; Munslow, I. J.; Sanders, C. J.; Scott, P. *Inorg. Chem.* **1999**, *38*, 3651–3656. (c) Scott, P.; Hitchcock, P. B. *Dalton Trans.* **1995**, 603–609.

(25) (a) Brinkman, E. A.; Berger, S.; Brauman, J. I. *J. Am. Chem. Soc.* **1994**, *116*, 8304–8310. (b) Hopkinson, A. C.; Lien, M. H. *J. Org. Chem.* **1981**, *46*, 998–1003.

Chart 2

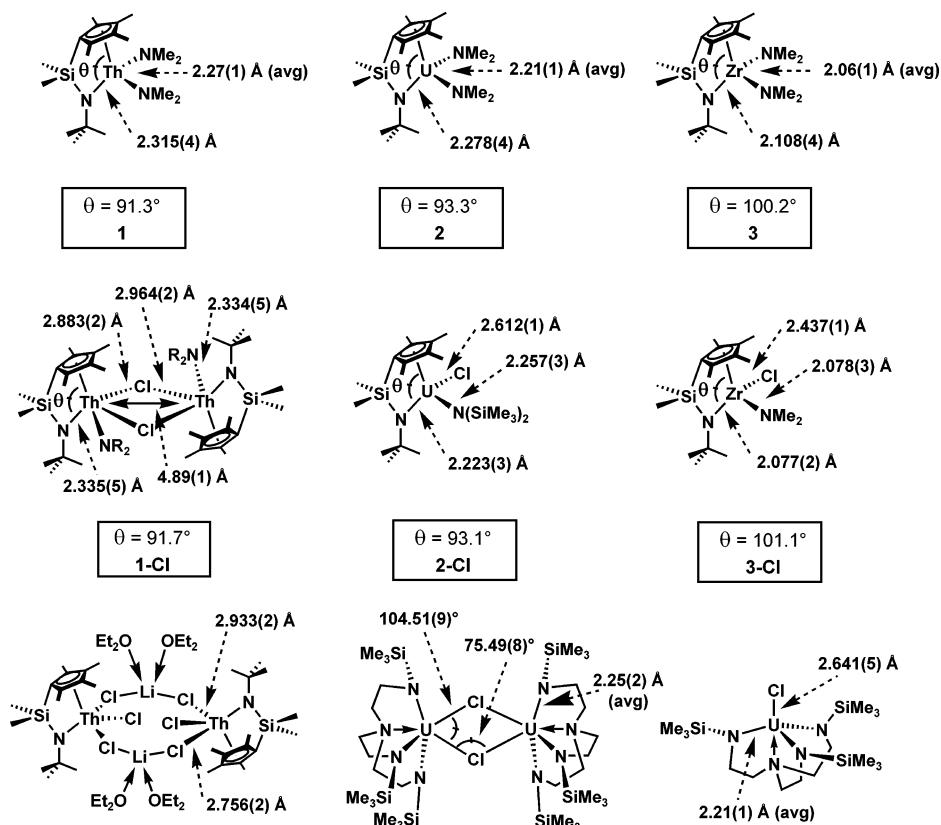
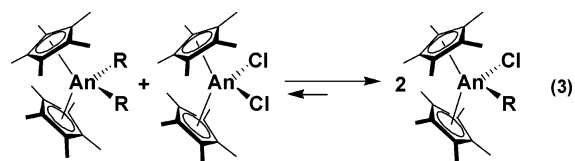


exhibit near-identical catalytic properties vs isolated precatalysts, and neither byproduct (CGC)Th(OAr)<sub>2</sub> nor unreacted ArOH significantly affects measured HA/cyclization  $N_t$  values, allowing convenient precatalyst generation. In the solid state, **1-OAr** is monomeric and crystallizes in space group  $P2_1/c$ , displaying a pseudotetrahedral coordination geometry (Figure 1d). The near-linear  $166.5(2)^\circ$  Th–O–C<sub>ipso</sub> angle and Th–O distance of 2.258(5) Å in **1-OAr** are characteristic of the large  $-O-2,6\text{-}i\text{Bu}_2\text{C}_6\text{H}_3$  moiety (Chart 3).<sup>29</sup> Cp'An(OAr)<sub>n</sub>R<sub>3-n</sub> complexes display An–O–C<sub>ipso</sub> angles in the range  $153.5(10)^\circ$ – $171.4(5)^\circ$ , along with An–O distances ranging 2.14(1)–2.189(6) Å (Th<sup>4+</sup>)<sup>29a,b</sup> and 2.135(4)–2.29(1) Å (U<sup>4+</sup>).<sup>29c</sup> Again, the coordinative unsaturation imparted by the CGC ancillary ligation (Cp(centroid)–Th–N(*t*Bu) =  $90.4^\circ$ ) re-

flects the steric and electronic factors that promote unique catalytic properties in (CGC)M<sup>3+/4+</sup> complexes (Charts 3 and 4).<sup>3k,11,13,15,30</sup>

Related complexes **5-Cl** and **6-Cl** can be generated via traditional salt metathesis or an alternative redistributive synthesis (eq 3).<sup>17</sup> The equilibrium lies  $\geq 95\%$  to the right for R = CH<sub>3</sub>,<sup>9b,17</sup> although the present bulkier R = CH<sub>2</sub>SiMe<sub>3</sub> substituents undergo such conproportions more sluggishly. The



reverse disproportionation is therefore expected to be of minor significance and is not detected by <sup>1</sup>H NMR spectroscopy of either **5-Cl** or **6-Cl** over several days at 25 °C or while heating at 90 °C for >36 h. Moreover, addition of ca. 10–100 equiv of Lewis basic amine substrate likely forms a species such as **D** (eq 4; as in Cp'2Ln– catalysts),<sup>1d,3a,v</sup> suggesting further steric impediment to Cp'2An[N(H)R]Cl redistribution. Monomeric imidoactinide complexes are typically stabilized by sterically screening ancillary ligation, e.g., Cp'2An< as opposed to *ansa* scaffolds Me<sub>2</sub>SiCp''2An< and (CGC)An<, with more open

- (26) For recent reviews on the chemistry of 4f and 5f elements, see: (a) Burns, C. J.; Neu, M. P.; Boukhalfa, H.; Gutowski, K. E.; Bridges, N. J.; Rogers, R. D. In *Comprehensive Coordination Chemistry II*; Abel, E. W., Stone, F. G. A., Wilkinson, G., Eds.; Pergamon: New York, 1995; Vol. 4, pp 189–345. (b) Edelmann, F. T.; Freckmann, D. M. M.; Schumann, H. *Chem. Rev.* **2002**, *102*, 1851–1896. (c) Molander, G. A.; Dowdy, E. D. *Top. Organomet. Chem.* **1999**, *2*, 119–154. (d) Edelmann, F. T. *Angew. Chem., Int. Ed.* **1995**, *34*, 2466–88. (e) Edelmann, F. T. In *Comprehensive Organometallic Chemistry II*; Abel, E. W.; Stone, F. G. A.; Wilkinson, G., Eds.; Pergamon: New York, 1995; Vol. 4, pp 11–213. (f) Schaverien, C. J. *Adv. Organomet. Chem.* **1994**, *36*, 283–362.
- (27) Klooster, W. T.; Brammer, L.; Schaverien, C. J.; Budzelaar, P. M. H. *J. Am. Chem. Soc.* **1999**, *121*, 1381–1382.
- (28) For example, see: (a) Turner, L. E.; Thom, M. G.; Fanwick, P. E.; Rothwell, I. P. *Organometallics* **2004**, *23*, 1576–1593. (b) Rothwell, I. P. *Chem. Commun.* **1997**, 1331–1338. (c) Zambrano, C. H.; Profflet, R. D.; Hill, J. E.; Fanwick, P. E.; Rothwell, I. P. *Polyhedron* **1993**, *12*, 689–708. (d) Rothwell, I. P. *Acc. Chem. Res.* **1988**, *21*, 153–159. (e) Lateskey, S.; Keddington, J.; McMullen, A. K.; Rothwell, I. P.; Huffman, J. C. *Inorg. Chem.* **1985**, *24*, 995–1001 and references therein.
- (29) (a) Clark, D. L.; Grumbine, S. K.; Scott, B. L.; Watkin, J. G. *Organometallics* **1996**, *15*, 949–57. (b) Butcher, R. J.; Clark, D. L.; Grumbine, S. K.; Scott, B. L.; Watkin, J. G. *Organometallics* **1996**, *15*, 1488–96. (c) Berg, J. M.; Clark, D. L.; Huffman, J. C.; Morris, D. E.; Sattelberger, A. P.; Streib, W. E.; Van der Sluys, W. G.; Watkin, J. G. *J. Am. Chem. Soc.* **1992**, *114*, 10811–21.

- (30) For reviews of constrained geometry catalysts, see: (a) Gromada, J.; Carpentier, J.-F.; Mortreux, A. *Coord. Chem. Rev.* **2004**, *248*, 397–410. (b) Okuda, J. *Dalton Trans.* **2003**, 2367–2378. (c) Arndt, S.; Okuda, J. *Chem. Rev.* **2002**, *102*, 1953–1976. (d) Britovsek, G. J. P.; Gibson, V. C.; Wass, D. F. *Angew. Chem., Int. Ed.* **1999**, *38*, 428–447.

Chart 3

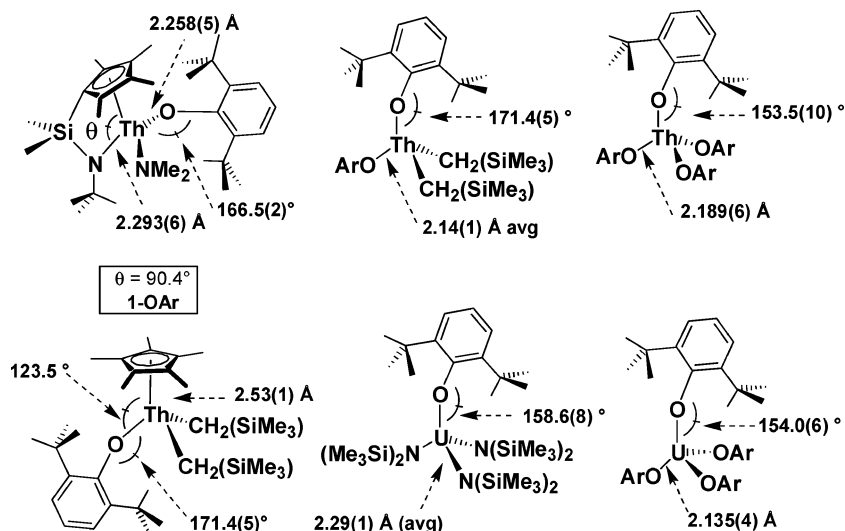
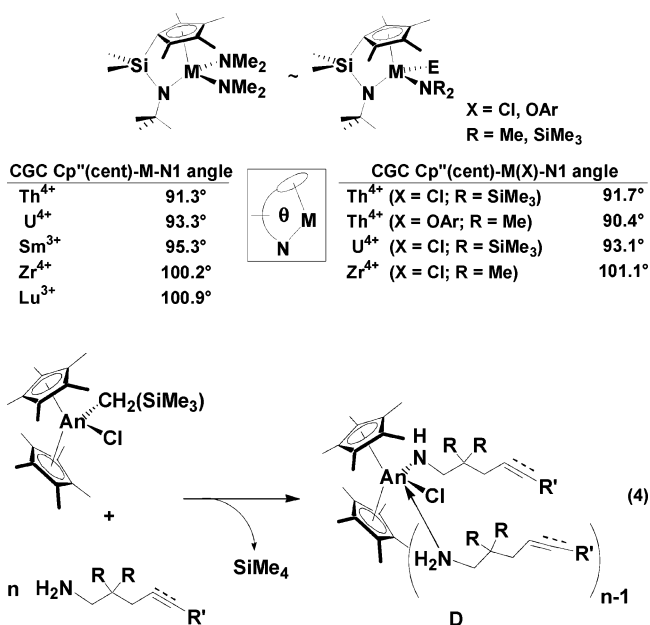
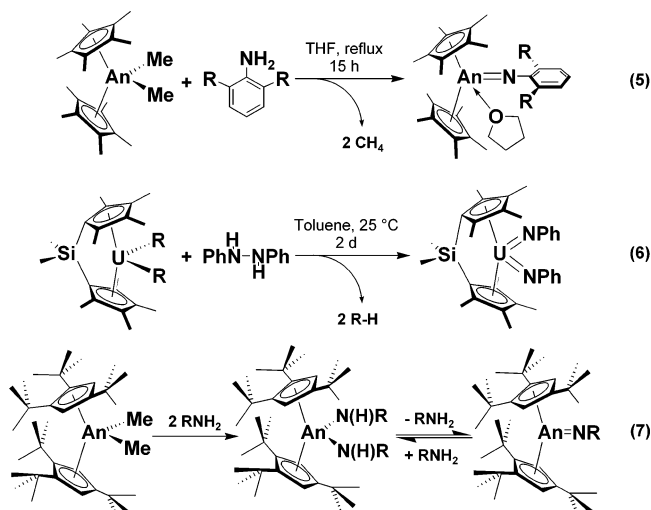


Chart 4



structures leading to dimeric/oligomeric species.<sup>26,31</sup> Imidoactinide complexes are generally formed under forcing conditions conducive to  $\alpha$ -elimination (e.g., eq 5) or under milder conditions employing reagents inducing oxidation to U<sup>6+</sup>, stabilizing more open coordination environments (e.g., eq 6). Computational studies implicate 6d and 5f orbital involvement in An=NR  $\pi$ -bonding with considerable positive charge at An (and negative charge buildup at =NR).<sup>32</sup> Moreover, L<sub>2</sub>An=NR complexes revert to bis(amido)actinide complexes in the pres-

ence of excess protic amines (e.g., (tBu<sub>3</sub>Cp)<sub>2</sub>An< in eq 7).<sup>31a</sup> Note that these synthetic routes appear generally inconsistent with the present catalytic reaction rates (25 °C, C<sub>6</sub>D<sub>6</sub>) and observed rate laws for aminoalkene and aminoalkyne HA/cyclizations (vide infra).



**Catalytic Intramolecular Hydroamination/Cyclization and Mechanistic Considerations.** In this section, the key features of the two most plausible mechanistic scenarios, i.e., C=C/C $\equiv$ C insertion into an M–N(H)R linkage (Scheme 1) vs formation of a reactive M=NR intermediate (Scheme 2), followed by C=C/C $\equiv$ C cycloaddition, are considered, followed by discussion of the data concerning intramolecular aminoalkyne and aminoalkene HA/cyclization pathways for representative primary and secondary amines mediated by (CGC)An< and (CGC)Zr< complexes. Effects of the metal ionic radius as well as  $\sigma$  and  $\pi$  ancillary ligation are discussed along with kinetic parameters for C=C and C $\equiv$ C unsaturations. L<sub>2</sub>An< catalysts are discussed first, followed by extension to (CGC)Zr< catalysts. We begin with a summary of relevant mechanistic observations.

**Summary of Mechanistically Relevant Results.** Below is a summary of the prominent features observed in HA/cyclization kinetic and catalytic activity studies with L<sub>2</sub>M(NR<sub>2</sub>)X catalysts 1–6.

(31) For examples of L<sub>2</sub>An=NR complexes and their reactivity, see: (a) Zi, G.; Blosch, L. L.; Jia, L.; Andersen, R. A. *Organometallics* **2005**, *24*, 4602–4612. (b) Arney, D. S. J.; Burns, C. J. *J. Am. Chem. Soc.* **1995**, *117*, 9448–60. (c) Brennan, J. G.; Andersen, R. A.; Zalkin, A. *J. Am. Chem. Soc.* **1988**, *110*, 4554–4558. (d) Morris, D. E.; DaRe, R. E.; Jantunen, K. C.; Castro-Rodriguez, I.; Kiplinger, J. L. *Organometallics* **2004**, *23*, 5142–5153. (e) Jantunen, K. C.; Burns, C. J.; Castro-Rodriguez, I.; DaRe, R. E.; Golden, J. T.; Morris, D. E.; Scott, B. L.; Taw, F. L.; Kiplinger, J. L. *Organometallics* **2004**, *23*, 4682–4692.

(32) (a) Bursten, B. E.; Strittmatter, R. J. *Angew. Chem., Int. Ed.* **1991**, *30*, 1069–1085. (b) Pepper, M.; Bursten, B. E. *Chem. Rev.* **1991**, *91*, 719–741. (c) Burns, C. J.; Bursten, B. E. *Comments Inorg. Chem.* **1989**, *9*, 61–93.

**Table 5.** Reported Mechanistic Characteristics of Various Hydroamination Pathways

	M–N(R)R (Schemes 1,3) intramolecular HA	M=NR (Scheme 2) intermolecular HA
rate law	$\nu \sim [M]^1[N-H]^0$ <sup>a</sup>	$\nu \sim [M]^1[N-H]^{-1}[\text{alkyne}]^1$ <sup>b</sup>
induction period?	no	yes
high [substrate]	no effect	rate decrease
low [substrate]	no effect	rate increase
high [product]	rate decrease <sup>c</sup>	~no effect <sup>c</sup>
$\Delta H^\ddagger$	~10 kcal/mol	~12 kcal/mol <sup>d</sup>
$\Delta S^\ddagger$	~–30 eu	~–45 eu <sup>d</sup>
C–C substitution dependence?	yes	yes (M = Zr) no (M = An)
2° amine substrates?	yes	no

<sup>a</sup> For intramolecular hydroamination/cyclization. <sup>b</sup> The rate law  $\nu \sim [M]^1[N-H]^0[\text{alkyne}]^0$  is predicted for the scenario depicted in eq 8b. Cp<sub>2</sub>An<-catalyzed *intermolecular* HA:  $\nu \sim [M]^1[N-H]^{-1}[\text{alkyne}]^0$ . <sup>c</sup> Bulky products unable to induce competitive binding/inhibition. <sup>d</sup> Measured for Cp<sub>2</sub>AnMe<sub>2</sub>-catalyzed *intermolecular* alkyne HA.

(i) Substituted (CGC)M(NR<sub>2</sub>)X-derived catalysts are frequently more active than their traditional (CGC)MR<sub>2</sub> counterparts (Tables 3–5).

(ii) Complete precatalyst activation by primary amine substrates occurs within seconds at –78 °C in toluene-*d*<sub>8</sub> solutions, and bulkier secondary amine substrates are rapidly activated under HA/cyclization catalysis conditions. Induction periods are not observed with L<sub>2</sub>MR<sub>2</sub> or L<sub>2</sub>M(R)X precatalysts (M = Zr, Th, U).

(iii) The observed rate law  $\nu \sim [L_2M<]^1[\text{amine}]^0$  is the same for organo-4f-, (CGC)An<-, and (CGC)Zr<-catalyzed HA/cyclizations (*vide infra*). Competitive binding/product inhibition of catalytic turnover is sometimes observed at high product concentrations (Figures 2c–d, 3c).

(iv) Ionic radius/metal accessibility trends for aminoalkyne and aminoalkene HA/cyclization are conserved relative to known L<sub>2</sub>Ln- and L<sub>2</sub>An<-catalyzed reactions (Tables 3–5).

(v) Both primary and secondary amine substrates are efficiently cyclized under mild reaction conditions (Tables 3–5). Secondary aminoalkene HA/cyclization rates are *not* accelerated in more polar solvent media.

(vi) Solution-phase magnetic moments of major (diamagnetic or paramagnetic) catalyst species do not change upon precatalyst activation or during/after catalytic runs.

(vii) Activation parameters measured for (CGC)M<-catalyzed aminoalkyne and aminoalkene HA/cyclization are very similar for both (CGC)MR<sub>2</sub> and (CGC)M(NR<sub>2</sub>)X catalysts (M = Th, U, Zr). Moderate  $\Delta H^\ddagger$  and large negative  $\Delta S^\ddagger$  values are characteristic of all L<sub>2</sub>Ln- and (CGC)An<-catalyzed HA/cyclizations (*vide infra*; Table 6, Figures 2, 3).

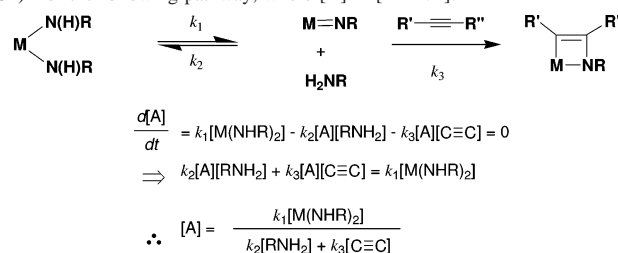
**Mechanistic Considerations.** As noted above, the two most plausible scenarios for intramolecular aminoalkene and aminoalkyne HA/cyclization are presented in Schemes 1 and 2 (Table 5). In the former, trivalent organolanthanides proceed through highly polar, highly organized insertive four-center transition states (Scheme 1, A). These reactions are characterized by moderate  $\Delta H^\ddagger$  (ca. 12 kcal/mol) and large negative  $\Delta S^\ddagger$  (ca. –30 eu) values, with their scope including primary and secondary amine substrates.<sup>1d,3o,v</sup> Although [amine] and [C–C] cannot be independently varied in *intramolecular* HA/cyclization kinetic studies, addition of noncyclizable competing Lewis bases (e.g., THF or *n*-propylamine) to intramolecular

reactions yields the rate law  $\nu \sim [L_2Ln-]^1[\text{base}]^{-1}$  for large [base]/[substrate], consistent with competitive inhibition of C=C/C≡C insertion.<sup>1d,3,4</sup> From similar arguments, an analogous pathway was proposed for L<sub>2</sub>Ln<sup>3+</sup>-mediated *intermolecular* HA of alkenes, alkynes, and dienes, with the observed rate law  $\nu \sim [\text{catalyst}]^1[\text{alkyne}]^1[\text{amine}]^0$ , consistent with turnover-limiting C–C insertion into an Ln–N bond, independent of amine exchange.<sup>1d,3f</sup> Note that zero-order [amine] dependence is expected for L<sub>2</sub>Ln– catalysts incapable of forming charge-neutral L<sub>2</sub>Ln=NR species and is consistent with immediate catalyst activation/initiation of turnover by substrate and secondary amine reactivity. Also, the marked *N<sub>i</sub>* dependence on ring size, substrate tether (α-alkyl and *gem*-dialkyl substitutions; Thorpe–Ingold effect),<sup>33</sup> and C–C substituent electronic effects (vs steric bulk) for alkene, alkyne, allene, and diene unsaturations argue strongly against turnover-limiting heterocycle protonolysis *after* C–C insertion into M–N (i.e.,  $k_{\text{protonolysis}} > k_{\text{insertion}}$  appears operative here).<sup>3a,x,5</sup>

The *intermolecular* HA pathway of Scheme 2 proceeds via L<sub>2</sub>M=NR intermediate **B** that undergoes [2 + 2] cycloaddition with disubstituted (reversible)<sup>8</sup> or terminal (irreversible)<sup>9</sup> alkynes. This process typically displays a brief induction period and rate law consistent with rapid pre-equilibrium loss of RNH<sub>2</sub>. Cp<sub>2</sub>Zr<-catalyzed reactions require bulky amines able to stabilize the Cp<sub>2</sub>Zr=NR intermediate, although excessive alkyne steric bulk is unnecessary (eq 8a). Cp<sub>2</sub>An<-mediated *intermolecular* alkyne HA,<sup>9</sup> complicated by concomitant alkyne oligomerization processes, behaves somewhat differently, exhibiting the rate law  $\nu \sim [\text{Cp}'_2\text{An}<]^1[\text{amine}]^{-1}[\text{alkyne}]^0$ . In each case, the nature of the amine substituents dictates rate and regioselectivity. Note that, although Cp<sub>2</sub>An< catalysts are active with less bulky aliphatic amines, secondary amine HA apparently does not proceed with either Cp<sub>2</sub>Zr< or Cp<sub>2</sub>An< catalysts. Interestingly, however, cationic (Et<sub>2</sub>N)<sub>3</sub>U<sup>+</sup>BPh<sub>4</sub><sup>–</sup> mediates the catalytic addition of secondary Et<sub>2</sub>NH to alkynes.<sup>9a</sup> Although inconsistent with synthetic L<sub>2</sub>An=NR chemistry for sterically open ligands,<sup>26,31</sup> an alternative scenario where an M=NR species forms *irreversibly*, followed by rapid C≡C addition, is conceivable (eq 8b).<sup>34</sup> Key features and mechanistic implications

(33) (a) Jung, M. E.; Pizzzi, G. *Chem. Rev.* **2005**, *105*, 1735–1766. (b) Sammes, P. G.; Weller, D. J. *Synthesis* **1995**, 1205–22.

(34) For the following pathway, where [A] = [M=NR]:

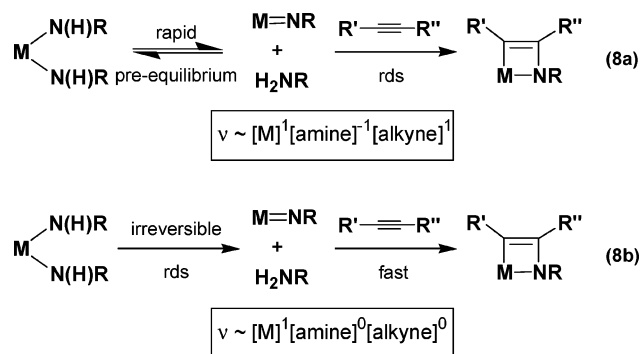


If the rate of product formation is

$$\nu = k_3[A][\text{C}\equiv\text{C}],$$

$$\text{then } \nu = \frac{k_1 k_3 [M(\text{NHR})_2][\text{C}\equiv\text{C}]}{k_2 [\text{RNH}_2] + k_3 [\text{C}\equiv\text{C}]}$$

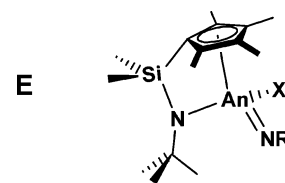
- Therefore:
- (i) for  $k_3$  very large,  $\nu \sim [M(\text{NHR})_2]^1[\text{RNH}_2]^0[\text{C}\equiv\text{C}]^0$
  - (ii) for  $k_2$  very large,  $\nu \sim [M(\text{NHR})_2]^1[\text{RNH}_2]^{-1}[\text{C}\equiv\text{C}]^1$
  - (iii) for  $k_3$  very small,  $\nu \sim [M(\text{NHR})_2]^1[\text{RNH}_2]^{-1}[\text{C}\equiv\text{C}]^1$



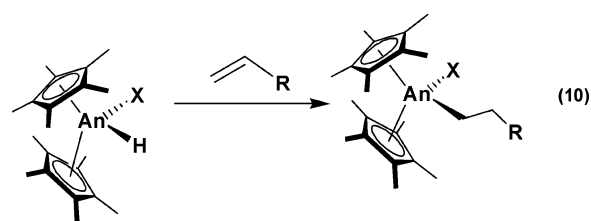
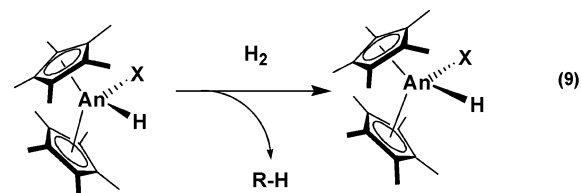
that would distinguish  $\sigma$ -bonded M–N(H)R vs  $\pi$ -bonded M=NR  $L_2M$ -catalyzed HA pathways based on mechanistic observations on  $L_2Ln$ - and  $Cp_2Zr$ - and  $L_2An$ - catalysts are summarized in Table 5. Beyond observed rate laws, the most strikingly different mechanistic characteristics concern the presence of an induction period, during which catalyst generation occurs (eq 8a), and an intrinsic inability to turn over secondary amines (vide infra) via an M=NR pathway. This scenario also exhibits a rate *increase* at low [amine] and rate *decrease* at high [amine], owing to inhibition of M=NR formation during the rapid pre-equilibrium (eq 8a). While an M–N(H)R pathway mediates secondary N–H bond addition to C–C unsaturations, competitive binding/product inhibition can sometimes lead to moderate rate depression at high [product]. Note that although inconsistent with observed reactivity trends and facile cyclization of secondary amine substrates,<sup>11b</sup> the seemingly less likely case of turnover-limiting heterocycle protonolysis following rapid C–C insertion/extrusion (i.e.,  $k_{insertion} > k_{protonolysis}$ ) simplifies the predicted rate law in eq 8a to  $v \sim [M]^1[alkyne]^1$ .

**Ligand and Metal Effects.** Intramolecular aminoalkyne HA/cyclization mediated by unsubstituted organoactinide complexes **1**, **2**, and **4–6** is broad in scope, with activity and selectivity dependent on the  $An^{4+}$  ionic radius and ancillary ligation.<sup>11</sup> For less open  $Me_2SiCp''_2An$ - and  $Cp'_2An$ - complexes, primary N–H bond addition to terminal and disubstituted aminoalkyne substrates is generally more rapid for Th than for U complexes. The rate disparity is greatest for hindered metallocene  $Cp'_2An$ - frameworks and least for more coordinatively unsaturated  $Me_2SiCp''_2An$ - frameworks. Similar rate dependences on ancillary ligation are observed for  $Ln^{3+}$  catalysts, where *smaller*  $Ln^{3+}$  ions and less accessible metal centers yield more active catalysts. In contrast to organo-4f catalysts, trends for (CGC)An< complexes **1** and **2** typify the enhanced aminoalkyne catalytic activity imparted by CGC ancillary ligation,<sup>30</sup> with far greater catalytic efficiency for (CGC)An< vs *less* open  $L_2An$ - complexes. Here the smaller  $U^{4+}$  ion in **2** achieves the most impressive  $N_t$  values, typically 10–100 $\times$  greater than that for organothorium complex **1**, retaining the ionic radius dependence observed with 4f catalysts and suggesting an intricate balance between coordinative unsaturation, metal ionic radius, bond covalency, and ligand/substrate electronic demands in organoactinide-mediated aminoalkyne HA/cyclization.<sup>11</sup>

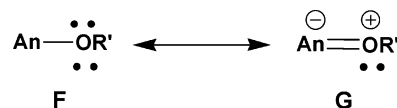
In the present study, (CGC)M(NR<sub>2</sub>)X-derived complexes (X = Cl, aryloxide) were investigated because the corresponding imido complexes (**E**) should not be readily accessible. It was found that HA/cyclization rates are generally comparable to or greater than those mediated by (CGC)M(NR<sub>2</sub>)<sub>2</sub> precatalysts, and within the context of a Schemes 1, 3 scenario, the question then



arises as to what effects are expected from the X ligand. Alkyl hydrogenolysis and An–H olefin insertion processes have been investigated for  $Cp'_2An(R)X$  complexes as a function of R and X (X = OR', Cl; eqs 9, 10).<sup>35</sup> Here, electron-donating alkoxide



coligands result in marked depression of reactivity, likely reflecting –OR'  $\pi$ -donation effects on An electrophilicity (cf., resonance forms **F** and **G**) as well as steric impediments. Parallel



trends are observed in both stoichiometric and catalytic  $Cp'_2An(R)Cl$  complex reactivity, consistent with Cl-based  $\pi$ -donation effects.<sup>32</sup> Computational and PES experiments also indicate a strong dependence of non-Cp ligand  $\sigma$ -/ $\pi$ -donor properties on the extent of bond covalency in actinocenes and argue that interactions with actinide 6d orbitals dominate  $\pi$ -bonding, consistent with observed effects on reactivity of electron-withdrawing X substituents.<sup>32</sup>

While monoamido complexes **1-Cl**, **2-Cl**, **1-OAr**, and **2-OAr** are effective precatalysts for aminoalkyne HA/cyclization, reactivity trends for  $L_2An(R)X$  complexes appear dependent on a variety of factors, and direct comparisons of X effects are complicated by the interplay between steric and electronic factors.<sup>11b</sup> Given the impact of the  $An^{4+}$  ionic radius on intramolecular HA/cyclization rates ( $Th^{4+} > U^{4+}$  for aminoalkenes vs  $U^{4+} > Th^{4+}$  for aminoalkynes) and greater metal center access afforded by the open CGC ancillary ligand (vs  $Me_2SiCp''_2An$ - and  $Cp'_2An$ - catalysts),<sup>11b,30</sup> the HA/cyclization rate trends **1** > **1-Cl** > **1-OAr** and **2-Cl** > **2** > **2-OAr** observed for primary aminoalkene conversion **11**  $\rightarrow$  **12** (Table 3) are similar to previously observed trends upon increasing metal center accessibility. The pattern (CGC)An(NMe<sub>2</sub>)<sub>2</sub> > (CGC)-

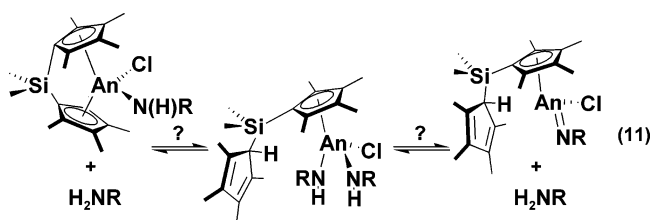
(35) (a) Lin, Z.; Marks, T. J. *J. Am. Chem. Soc.* **1990**, *112*, 5515–5525. (b) Lin, Z.; Le Marechal, J.-F.; Sabat, M.; Marks, T. J. *J. Am. Chem. Soc.* **1987**, *109*, 4127–4129. (c) Lin, Z.; Marks, T. J. *J. Am. Chem. Soc.* **1987**, *109*, 7979–7985.

**Table 6.** Experimental Activation Parameters for Intramolecular Aminoalkene and Aminoalkyne HA/Cyclization Catalyzed by Cp'<sub>2</sub>Ln-, (CGC)An<, and (CGC)Zr< Complexes at ≥40 °C Temperature Range in C<sub>6</sub>D<sub>6</sub>

unsaturation	precatalyst	substrate	$\Delta H^\ddagger$ (kcal/mol)	$\Delta S^\ddagger$ (eu)	$E_a$ (kcal/mol)	ref
aminoalkene	Cp' <sub>2</sub> La[CH(SiMe <sub>3</sub> ) <sub>2</sub> ]	R = R' = R'' = H, n = 1	12.7(5)	-27(2)	13.4(5)	3v
	(CGC)Th(NMe <sub>2</sub> ) <sub>2</sub>	R = Ph, R' = R'' = H, n = 2	12.6(5)	-30(1)	13.3(7)	11b
	(CGC)U(NMe <sub>2</sub> )OAr	R = Ph, R' = R'' = H, n = 1 ( <b>11</b> )	10(3)	-43(9)	11(3)	this work
2° aminoalkene	(CGC)Th(NMe <sub>2</sub> ) <sub>2</sub>	R = Ph, R' = H, R'' = Me, n = 1 ( <b>13</b> )	9(3)	-48(6)	10(3)	this work
aminoalkyne	Cp' <sub>2</sub> Sm[CH(SiMe <sub>3</sub> ) <sub>2</sub> ]	R = R' = R'' = H, n = 1	11(8)	-27(6)		3o
	(CGC)Th(NMe <sub>2</sub> ) <sub>2</sub>	R = R'' = H, R' = Me, n = 1 ( <b>9</b> )	14(2)	-27(5)	15(2)	11b
	(CGC)U[N(SiMe <sub>3</sub> ) <sub>2</sub> ]Cl	R = R'' = H, R' = Me, n = 1 ( <b>9</b> )	16(3)	-18(9)	17(3)	this work
	(CGC)Zr(NMe <sub>2</sub> )Cl	R = R'' = H, R' = SiMe <sub>3</sub> , n = 1 ( <b>7</b> )	11(2)	-35(7)	12(2)	this work

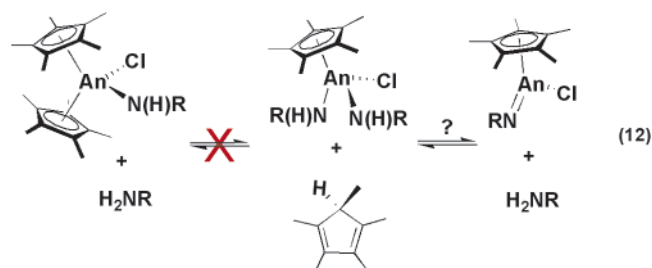
An(NMe<sub>2</sub>)Cl > (CGC)An(NMe<sub>2</sub>)OAr observed for **13** → **14** HA/cyclization (Table 4) is consistent with diminished importance of the An<sup>4+</sup> ionic radius with *secondary* aminoalkene substrates and reflects the substantial steric crowding afforded by the 2,6-di-*tert*-butylphenoxide ligand for an already congested C=C insertion into an M–N(R')R bond (cf., R<sup>3</sup> ≠ H in **C**, Scheme 3). Note that although CGC-imposed geometric constraints are uniform, the presence of a relatively small, relatively nonlabile chloride ligand as opposed to an encumbered, substrate-derived amido moiety should reduce HA transition state steric congestion. For aminoalkyne HA/cyclization, the general trend **1-Cl** > **1** > **1-OAr** is observed for An = Th, while trends for An = U (i.e., **2** > **2-Cl** > **2-OAr**, R = SiMe<sub>3</sub>, **7** → **8**; **2** > **2-OAr** > **2-Cl**, R = Me, **9** → **10**) vary with alkyne substitution (Table 2), providing additional evidence for increased importance of transition state electronic demands in aminoalkyne HA/cyclization.<sup>1d,3,4,11b</sup> This is also seen with secondary aminoalkyne cyclization **15** → **16**, where the less hindered chloride ligand effects less rapid N<sub>t</sub> with (CGC)M–(NR<sub>2</sub>)Cl for M = Zr, Th, U, though (CGC)An< complexes retaining their reactivity advantage<sup>11,30</sup> over Cp'<sub>2</sub>An< catalysts (Table 4). Interestingly, with the exception of **15** → **16**, monoamido zirconium precatalyst **3-Cl** is a more efficient precatalyst than **3** in mediating the aminoalkene and aminoalkyne transformations investigated here, suggesting that decreased steric hindrance outweighs electronic demands for Zr-mediated *intramolecular* HA/cyclization.

Metallocenes **4/4-Cl** (Me<sub>2</sub>SiCp''<sub>2</sub>U<), **5/5-Cl** (Cp'<sub>2</sub>Th<), and **6/6-Cl** (Cp'<sub>2</sub>U<) were also investigated as precatalysts in *aminoalkyne* **7** → **8** HA/cyclization. The catalytic activity of *ansa*-metallocenes **4** and **4-Cl** is largely unaffected by chloride incorporation. However, potential Cp'' ring detachment (eq 11),



previously observed for mixed-ring organolanthanide catalysts,<sup>3r,s</sup> prompted a more thorough investigation of the Cp'<sub>2</sub>AnR<sub>2</sub>

precatalysts, where reversible ring dissociation is less likely.<sup>17,36</sup> GC/MS and <sup>1</sup>H NMR analyses of reaction mixtures during and immediately following **7** → **8** cyclization give no sign of HCp' or single-ring Cp'An< species, arguing that ring protonolysis is unlikely (eq 12). Interestingly, a 100× decrease in activity



is observed in these complexes vs Cp'<sub>2</sub>An< for conversion **7** → **8** (Table 2), perhaps reflecting the pronounced deactivation by the chloride ligand electronic characteristics as discussed above for An–R hydrogenolysis/An–H olefin insertion processes (eq 9, 10).<sup>35</sup> Decreased electrophilicity could reduce alkyne insertion rates, depressing N<sub>t</sub> vs Cp'<sub>2</sub>An<, Me<sub>2</sub>SiCp''<sub>2</sub>An<, and (CGC)An< catalysts.<sup>37</sup> Alternatively, the agency of Cp'<sub>2</sub>An=NR species in the sterically protected Cp'<sub>2</sub> environment could explain diminished reactivity vs more open ancillary ligation favoring M–N(H)R intermediates, especially in light of the reported difficulty of cycloloading C=C bonds to M=NR bonds (M = Ti, Zr).<sup>1,10</sup> However, that Cp'<sub>2</sub>An< complexes mediate *intramolecular* aminoalkyne HA/cyclization of primary and secondary amines with zero-order dependence on [amine] and without protonolytic HCp' release argues for a σ-bonded M–N insertive pathway, even in sterically congested environments.

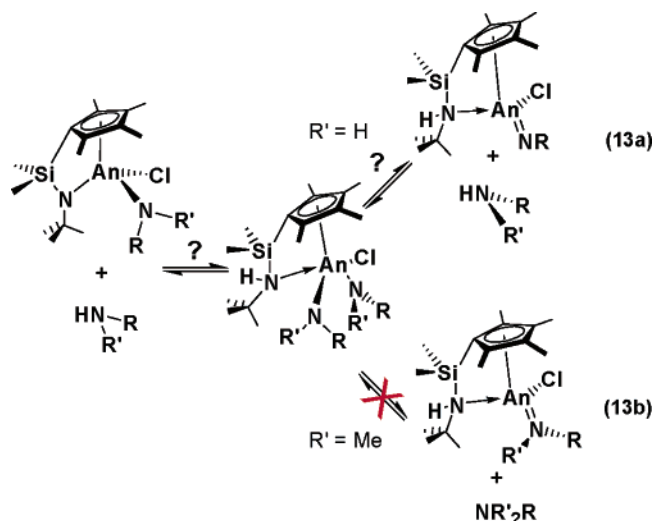
A ligand dissociation/reattachment process analogous to eqs 11 and 12 is in principle possible with CGC ancillary ligation (eq 13). Although not spectroscopically observed, the chelating (tBu)N–An<sup>4+</sup> moiety in (CGC)An< complexes could be displaced in the presence of a large excess of substrate

(36) (a) Arduini, A. L.; Edelstein, M.; Jamerson, J. D.; Reynolds, J. G.; Schimid, K.; Takats, J. *Inorg. Chem.* **1981**, *20*, 2470–2474. (b) Fagan, P. J.; Manriquez, J. M.; Vollmer, S. H.; Day, C. S.; Day, V. W.; Marks, T. J. *J. Am. Chem. Soc.* **1981**, *103*, 2206–2220.

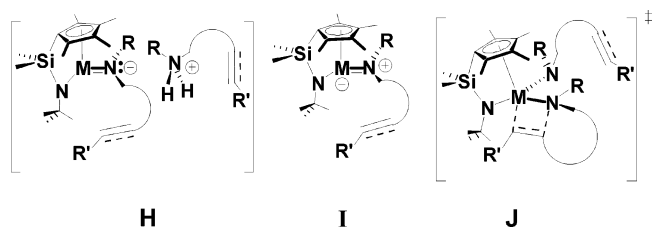
(37) (a) Lanza, G.; Fragala, I. L.; Marks, T. J. *Organometallics* **2002**, *21*, 5594–5612. (b) Lanza, G.; Fragala, I. L.; Marks, T. J. *Organometallics* **2001**, *20*, 4006–4017. (c) Lanza, G.; Fragala, I. L.; Marks, T. J. *J. Am. Chem. Soc.* **2000**, *122*, 12764–12777.



molecules, enabling transient  $An=NR$  formation (eq 13a,  $R' = H$ ) and, potentially,  $C=C/C\equiv C$  [2 + 2] cycloaddition. However, the catalytic activity of *any*  $L_2M<$  complex with secondary amine substrates (eq 13b,  $R' \neq H$ ) with observed rate law  $v \sim [M]^1[amine]^0$  provides compelling evidence for an insertive M–N( $R'$ )R pathway (Scheme 3), and the comparable competence of substituted and unsubstituted **1–2** in mediating such transformations argues that an  $L_2An=NR$  imidoactinide intermediate (**B**) is not catalytically important here. Passage through an



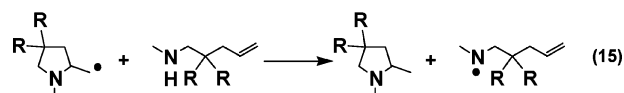
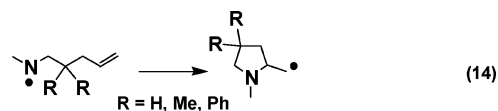
$L_2M=NR$  reactive intermediate requires an unprecedented high-energy species similar to **H** or **I** in lieu of the more reasonable **J**. Saltlike structure **H** would presumably be generated via  $\alpha$ -hydrogen abstraction<sup>8,9,38</sup> and involves hypervalent N bonded directly to  $M^{4+}$ , whereas zwitterionic **I** (via electron pair transfer from N to the An–N bond) places a formal negative charge on  $An^{4+}$  or  $Zr^{4+}$  (no change in diamagnetism or  $\mu_{eff}$  is observed during primary or secondary amine HA/cyclization). Moreover,



species **H** or **I** should be stabilized in more polar media, contrary to the observed  $N_t$  decrease for **2** (rapid catalyst decomposition occurs with **1**). Also note that the high yields and regioselectivity in the present aminoalkene and aminoalkyne HA/cyclizations are inconsistent with radical (chain) processes (eqs 14, 15).<sup>39</sup> The required but energetically unfavorable  $An^{4+} \rightarrow An^{3+}$  electron transfer/reduction process (particularly for  $An = Th$ ),<sup>26</sup> rate dependence on the metal ionic radius, zero-order dependence on [substrate],<sup>20</sup> and pronounced effects of ancillary ligation on  $N_t$  and diastereoselectivity all render radical pathways that are unlikely, particularly in light of reported trends in

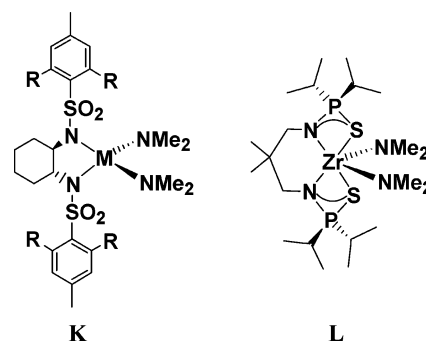
(38) An analogous mechanism is invoked in imidotitanium synthesis: Hazari, N.; Mountford, P. *Acc. Chem. Res.* **2005**, *38*, 839–849.

(39) (a) Walton, J. C.; Studer, A. *Acc. Chem. Res.* **2005**, *38*, 794–802. (b) Kemper, J.; Studer, A. *Angew. Chem., Int. Ed.* **2005**, *44*, 4914–4917. (c) Newcomb, M.; Burchill, M. T.; Deeb, T. M. *J. Am. Chem. Soc.* **1988**, *110*, 6528–6535.



heterocycle yield and regioselectivity in radical-mediated aminoalkene cyclizations.<sup>39b,c</sup>

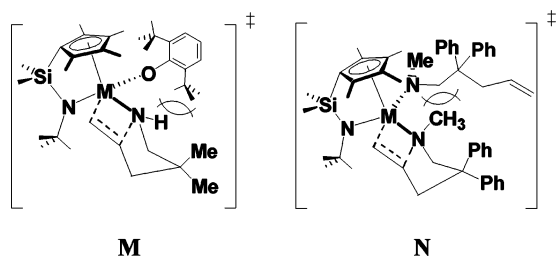
**(CGC)Zr<-Mediated Hydroamination.** Initial intramolecular aminoalkyne HA/cyclization reports have proposed the involvement of in situ generated  $CpM=NR(Cl)$  species ( $M = Ti, Zr$ ) at high catalyst loadings ( $\geq 20$  mol %), starting from  $CpM(CH_3)_2Cl$  or  $CpMCl_3$  with 40 mol %  $iPr_2NEt$  in THF.<sup>7f,g</sup> More recently, well-defined group 4 amidate, metallocene, and chelating diamide complexes have been applied to primary aminoalkyne (**K**;  $M = Ti, Zr$ ;  $R = H, Me$ )<sup>7b</sup> and aminoalkene (**L**; 120–150 °C) HA/cyclizations, invoking similar  $M=NR$  pathways.<sup>6d</sup> Sterically open homoleptic  $Ti(NMe_2)_4$  also mediates



intramolecular primary aminoalkene HA/cyclization.<sup>6e</sup> Although it is again reasonable to expect electron-withdrawing chloride ligands to reduce catalytic activity,<sup>35</sup> substituted **3-Cl** is typically the more efficient (CGC)Zr< precatalyst found in this study. For the  $Me_3Si$ -substituted aminoalkyne conversion **7**  $\rightarrow$  **8**, this difference is quite pronounced (Table 2), and for transformations **9**  $\rightarrow$  **10** and **11**  $\rightarrow$  **12** (Tables 3, 4), the distinction is again significant, displaying a roughly 2- to 3-fold enhancement vs complex **3**. The activities of **3-Cl** and **3** in mediating **11**  $\rightarrow$  **12** at 100 °C are roughly 4 $\times$  and 2 $\times$  greater, respectively, than electron-rich precatalyst **L**<sup>6d</sup> ( $Ti(NMe_2)_4$  is ca. 2 $\times$  less active than **L**).<sup>6e</sup> Secondary amine **13**  $\rightarrow$  **14** and **15**  $\rightarrow$  **16** HA/cyclizations mediated by (CGC)Zr< are considerably more sluggish than those with (CGC)An< catalysts, reflecting metal accessibility effects on  $N_t$ .<sup>1,3,11b</sup> The added steric hindrance in secondary vs primary aminoalkenes **13** (Table 4) and **11** (Table 3), where cyclization rates are comparable, is offset by the enhanced transition state orientation (Thorpe–Ingold effect)<sup>33</sup> of substrate chain *gem*-diphenyl vs *gem*-dimethyl groups. Furthermore, in light of the similar catalytic behavior of (CGC)An< and (CGC)Zr< catalysts, the  $N_t$  trends (**3-Cl** > **3** for **11**  $\rightarrow$  **12** vs **3** > **3-Cl** for **15**  $\rightarrow$  **16**) presumably reflect the importance of transition-state steric demands, where the small, rigid chloride ligand provides a less hindered site for  $C=C/C\equiv C$  insertion, perhaps outweighing electronic deactivation (cf., Scheme 1, **A** and Scheme 3, **C**). In addition, while cationic group 3 catalysts mediate intramolecular primary aminoalkene HA/cyclization,<sup>4a,h</sup> and  $Cp_2ZrMe^+MeB(C_6F_5)_3^-$  effects more

thermodynamically favorable<sup>1</sup> primary aminoallene HA/cyclization,<sup>7b</sup> cationic  $L_2M(R)^+XB(C_6F_5)_3^-$  ( $M = Ti^{4+}, Zr^{4+}$ ;  $R = Me, CH_2Ph$ ;  $X = C_6F_5$ , R) catalysts are *only* active for secondary amine intramolecular HA/cyclizations.<sup>10</sup> Interestingly, the poisoning of these cationic catalysts by primary amine substrates has been rationalized as deactivation via *unreactive* neutral imido complex formation.<sup>8–10,38</sup> Taken together, these observations, in conjunction with the present results, argue that it is not necessary to invoke  $M=NR$  intermediates in intramolecular HA/cyclization reactions mediated by organozirconium catalysts and that a  $\sigma$ -bonded  $M-N$  mechanistic pathway is accessible and perhaps *favoured*.

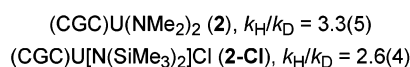
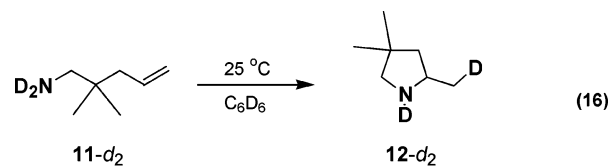
**Activation Parameter Parallels.** Activation parameters determined for intramolecular HA/cyclization mediated by monoamido (CGC) $M(NR_2)X$  catalysts ( $M = An, Zr$ ) are comparable to those for similar processes mediated by  $L_2AnR_2$  and  $L_2LnR$  catalysts (Table 6). The moderate  $\Delta H^\ddagger$  and large negative  $\Delta S^\ddagger$  values are consistent with highly ordered  $C=C/C\equiv C$  insertive transition states having considerable bond-forming accompanying bond-breaking.<sup>40</sup> The change in  $\Delta S^\ddagger$  to more negative values with  $11 \rightarrow 12$  conversion mediated by **2-OAr** ( $\Delta S^\ddagger = -43(9)$  eu) is consistent with the transition state ordering necessary to accommodate the steric hindrance of the large aryloxy ligand (**M**; cf., C, Scheme 3). A similar change in  $\Delta S^\ddagger$  for HA/cyclization  $13 \rightarrow 14$  mediated by **1** ( $\Delta S^\ddagger = -48(6)$  eu) is also not surprising given the nonbonding repulsions engendered by the *N*-methyl group of **13** and substrate organization required prior to  $C=C$  insertion (**N**; cf., C, Scheme 3). To our knowledge, activation parameters have not been reported for group 4 mediated HA/cyclizations,<sup>1,6,7</sup> although *intermolecular* terminal alkyne + aliphatic amine HA mediated by  $Cp'_2AnMe_2$  also displays comparable parameters,  $\Delta H^\ddagger = 11.7(3)$  kcal/mol and  $\Delta S^\ddagger = -44.5(8)$  eu.<sup>41</sup> That the present



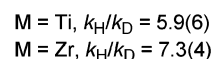
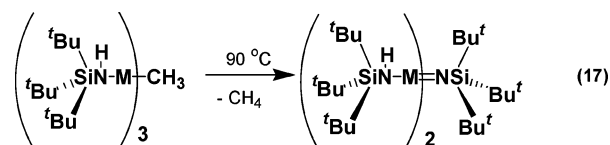
activation parameters parallel those for  $L_2Ln-$  and  $L_2An<$ -catalyzed HA/cyclizations<sup>1d,3,11</sup> suggests that the mechanism and turnover-limiting steps in each process are very similar if not identical. Zero-order substrate kinetic dependence, characteristic of intramolecular HA (Table 5),<sup>1</sup> indicates that a rapid pre-equilibrium involving  $RNH_2$  extrusion is *not* significant, while the ready cyclization of secondary amine substrates argues against the involvement of conventional  $M=NR$  species produced via  $\alpha-H$  elimination.

**Kinetic Isotope Effects.** In a similar organolanthanide aminoalkene HA/cyclization, substantial deuterium KIEs are observed in the range  $k_H/k_D = 2.7(4)–5.2(8)$ , varying with substrate structure and temperature from 25 to 60 °C,<sup>3v</sup> while

an analogous  $k_H/k_D = 4.2$  is reported at 40 °C for chiral binaphtholate  $Ln$  complexes.<sup>4b</sup> The marked HA/cyclization rate dependence on ring size and alkyl chain substitution in addition to other arguments<sup>1d</sup> suggest that the significant  $N-H/N-D$  KIE does *not* result from turnover-limiting protonolysis of completely cyclized aminoalkene but rather that protonolysis may be concurrent with cyclization. In the present study, the observed  $k_H/k_D = 3.3(5)$  and  $2.6(4)$  for **2** and **2-Cl**, respectively, are in excellent agreement with  $Ln$ -mediated aminoalkene HA/cyclization results (eq 16), further supporting an  $M-N$   $\sigma$ -bonded mechanistic pathway (Scheme 1). To our knowledge, similar



KIE studies have not been reported in group 4 catalysts, where aminoalkene HA is typically sluggish, limiting direct comparisons with organolanthanide catalysts. However, in the unimolecular  $\alpha$ -elimination process shown in eq 17, where an  $M=NR$  species is generated with bulky  $R = Si^t(Bu)_3$  groups, a significantly larger KIE is observed with  $k_H/k_D = 5.9(6)$  and  $7.3(4)$  for  $M = Ti, Zr$ , respectively.<sup>42</sup> This stark contrast in



$N-H/N-D$  KIEs suggests that unimolecular  $M=NR$  formation is not significant in the turnover-limiting step of (CGC) $An<$ -mediated intramolecular HA/cyclization.

**Mechanistic Summary.** It is useful to briefly summarize the observations supporting the basic HA/cyclization pathway of Scheme 3. The present (CGC) $M<$  catalysts could reasonably mediate intramolecular HA/cyclization via either of two plausible mechanistic scenarios: (1) a highly polar, highly organized four-centered, insertive transition state involving catalytically active (CGC) $M<$  species possessing two  $M-N(H)R$   $\sigma$ -bonds (“ $Ln$ -like”; Scheme 1) or (2) a [2 + 2] cycloaddition probably following a rapid pre-equilibrium (step (i), Scheme 2) that generates  $L_2M=NR$  reactive intermediate **B**. Note that stable monomeric  $L_2An=NR$  complexes invoked in scenario (2) are challenging synthetic targets (*vide supra*), particularly with unencumbered ancillary ligation,<sup>31</sup> and that imidoactinide complexes typically revert to bis(amido)actinides in the presence of excess amine (cf., eq 7b).<sup>31a</sup>

The data here support mechanistic scenario (1) (Scheme 3), with perhaps the strongest evidence opposing scenario (2) (eq 8; Scheme 2) being the ability of (CGC) $An(NMe_2)_2$ , (CGC)-

(40) (a) Illuminati, G.; Mandolini, L. *Acc. Chem. Res.* **1981**, *14*, 95–102. (b) Mandolini, L. *J. Am. Chem. Soc.* **1978**, *100*, 550–554.

(41) The experimentally determined  $\Delta S^\ddagger = -44.5(8)$  eu for intermolecular HA is representative of a bimolecular  $C\equiv C$  insertion process, as opposed to the unimolecular insertion proposed for intramolecular HA/cyclization ( $\Delta S^\ddagger$  ca.  $-30$  eu). See ref 1d for details.

(42) (a) Cummins, C. C.; Schaller, C. P.; Van Duyne, G. D.; Wolczanski, P. T.; Chan, A. W. E.; Hoffman, R. *J. Am. Chem. Soc.* **1991**, *113*, 2985–2994. (b) Cummins, C. C.; Baxter, S. M.; Wolczanski, P. T. *J. Am. Chem. Soc.* **1988**, *110*, 8731–8733.

ZrMe<sub>2</sub>, and (CGC)M(NR<sub>2</sub>)X precatalysts **1–6** to effectively mediate secondary *N*-alkyl aminoalkene and aminoalkyne HA/cyclizations. The relative depression in  $N_t$  for secondary vs primary substrates is consistent with trends previously observed for L<sub>2</sub>Ln– catalysts, where diminished turnover frequencies can be attributed to unfavorable steric interactions.<sup>1d,3,4</sup> In the present study, secondary amine HA/cyclizations proceed without deviation from the observed primary amine rate law,  $\nu \sim [L_2M<]^{-1}[amine]^0$ , and with similar activation energetics, arguing that a mechanistic scenario similar to Scheme 3 is again operative. While a pathway proceeding through an active L<sub>2</sub>M=NR species (**B**) is conceivable in unsubstituted L<sub>2</sub>MR<sub>2</sub> complexes with primary amine substrates, the mild reaction conditions, absence of required steric bulk in amine substrates, facile cyclization of 2° amine substrates, and lack of an induction period prior to catalytic turnover argue against scenario (2)/Scheme 2. Moreover, the [amine]<sup>–1</sup> kinetics seen in [2 + 2] cycloaddition pathways<sup>8</sup> differs from the present results, where high [product] sometimes depresses  $N_t$  owing to competitive binding/inhibition (Table 5).<sup>1d,3v,11</sup> Devoid of unlikely intermediates **H** or **I** and without detectable ancillary ligand detachment or rearrangement (eqs 2, 3, 11–13), there are no obvious pathways from L<sub>2</sub>M(NR<sub>2</sub>)X complexes **1–6** to the M=NR species required in scenario (2), making this pathway unlikely for either primary or secondary amine substrates.

## Conclusions

Catalytic intramolecular HA/cyclization reactions mediated by selectively substituted 5f and d<sup>0</sup> complexes provide strong

evidence for a mechanistic pathway proceeding via C=C/C≡C insertion at an M–N(H)R  $\sigma$ -bond (Schemes 1, 3), particularly with sterically open CGC ancillary ligation in the presence of excess amine substrate. The ability of (CGC)MR<sub>2</sub> and (CGC)M(NR<sub>2</sub>)X complexes to effectively promote HA/cyclization of *both* primary and secondary aminoalkyne and aminoalkene substrates with comparable rates and activation parameters argues that M=NR intermediates are unlikely and that a pathway involving insertion at an M–N  $\sigma$ -bonded intermediate is kinetically viable. Moreover, activities of selectively substituted (CGC)M(NR<sub>2</sub>)X complexes generally exceed those of (CGC)MR<sub>2</sub> precatalysts, further supporting passage through a transition state similar to **A** or **C** with a strong dependence on nonbonded interactions and C=C/C≡C insertion into an M–N(H)R  $\sigma$ -bonded intermediate (Scheme 3).

**Acknowledgment.** The National Science Foundation (CHE-0415407) is gratefully acknowledged for funding this research. We also thank Ms. C. L. Stern for assistance with X-ray diffraction data collection as well as Mr. M. R. Salata and Dr. A. K. Dash for helpful discussions.

**Supporting Information Available:** Full experimental details, including precatalyst syntheses, methods for kinetic studies, and X-ray diffraction analyses with Crystallographic Information Files and data tables for **1-Cl**, **2-Cl**, **3-Cl**, and **1-OAr**. This material is available free of charge via the Internet at <http://pubs.acs.org>.

JA0675898